AD

LOW VOLTAGE SCANNING ELECTRON MICROSCOPY

FINAL REPORT

by

Dr E D Boyes

OCTOBER 1988

United States Army

EUROPEAN RESEARCH OFFICE OF THE U.S. ARMY

London England

CONTRACT NUMBER DAJA 37-82-C-0271

UNIVERSITY OF OXFORD

Approved for Public Release; Distribution Unlimited

Acknowledgements

It is a pleasure to acknowledge the advice, support and assistance of several organisations and people.

The project was made possible with financial support provided by the :-

University of Oxford and the Department of Metallurgy and Science of Materials,

European Research Office of the United States Army,

Science and Engineering Research Council (SERC).

The advice, encouragement and support of the Head of the Department of Metallurgy and Science of Materials, Professor Sir Peter Hirsch FRS, were invaluable - and greatly appreciated - throughout the project.

Several members of the staff of the European Research Office, and of the associated laboratories, were instrumental in establishing and running the project; and all of them have made a significant contribution to it : Dr Robert Quattrone, Dr Fred Rothwarf, Dr Iqbal Ahmed and Dr Bill Simmonds. Dr Art Guenther and Major John Gowan (USAF) also contributed.

The practical work on the project progressed with the expert workshop assistance of John Stead in machining etc many of the fabrications needed for the unique LVSEM instrument.

Finally I should like to thank all of those many people who have come into contact with the LVSEM project, and particularly my colleagues in the Oxford Metallurgy Department, for their universally helpful and constructive attitude to the project.

Low Voltage Scanning Electron Microscopy

List of Keywords

Scanning electron microscopy
SEM
X-ray
Micoranalysis
EDX/EDS
Low voltage
High resolution
Ceramic surfaces
Supported catalysts
Metal particles
Field emission
Second zone lens
Digital imaging
Uncoated (SEM specimens)
Surface studies

Table of Contents

2. Summary : Low Voltage Scanning Electron Microscopy

Low voltage scanning electron microscopy has become an established technique over the last few years and our LVSEM project has made a major contribution to this process. There has been a series of publications and presentations, including the keynote paper at the 41st Annual Meeting of the Electron Microscopy Society of America (EMSA) in 1984. The author has been invited to present the results of the work in keynote talks at SEM West, to be held in San Diego, 4-7 April 1989, at an Institute of Physics meeting in London in February 1989 and at the combined EMAG/Micro-89 to be held in London in September 1989. LVSEM will also feature in the more general invited paper for EMSA in San Antonio in 1989.

At low voltages the beam-specimen interaction is modified, the range of beam penetration within the specimen is greatly reduced and the yield of secondary electrons is enhanced sufficiently to eliminate most of the severe charging and image distortion problems experienced with electrically non-conducting samples at higher voltages.

Experiments are continuing, with a series of specially fabricated test specimens and more practical samples, to explore the parameters which are important in determining both image contrast and the potential for enhanced microanalysis at low voltages in the range 0.5-5kV. In preliminary experiments, the spatial and depth resolution of EDX chemical microanalysis of bulk SEM specimens has been improved substantially.

There has been detailed study of the optical problems of low voltage operation, and the considerable potential which exists for improvements in the instrumentation; some of which have been published In the meantime the low voltage performance of conventional SEMs has been developed by the various manufacturers to achieve typically ~0.1μm at 1kV. The case for a dedicated LVSEM, able to challenge TEM resolution, remains strong.

The completion of the high specification test rig LVSEM instrument has been delayed by a series of technical problems, none of which has proved insurmountable, but which in total have extended the timescale beyond the end of the present contract.

The work should be extended with dedicated digital image processing, a specimen chamber upgraded to ultra-high vacuum (UHV) specification and a windowless EDX detector for chemical microanalysis with a predicted spatial resolution of <30nm using a beam energy <1kV.

4. ABSTRACT OF ORIGINAL PROPOSAL

Low Voltage Scanning Electron Microscopy

E D Boyes and P B Hirsch, Oxford University

A new type of surface scanning electron microscope (SEM) is proposed. It is designed to produce the first high resolution images of surfaces of uncoated non-conducting specimens such as ceramics, supported catalysts etc.

Very useful 5-20nm resolution images of surfaces are obtainable with a conventional electron microscope operated at 25-100kV but at these accelerating voltages the secondary electron yield of most materials is very low, typically <0.1, and there are therefore severe surface charging problems with non-conducting regions, the images of which are consequently of poor quality. Conversely at very low voltages of 1-3kV secondary electron yields are high and generally close to unity, minimising surface charging problems, but the electron-optical performance of the conventional microscope is limited to a resolution of about 0.2μm at 2kV. In many practical applications high voltages are used and the specimens are coated with a conducting metal film to control charging, but this reduces the potential for high resolution surface information and may complicate any subsequent microanalysis.

The proposed microscope is designed to improve substantially the low voltage imaging performance to about 5nm at 5kV and 10nm at 2kV. It is therefore expected to eliminate the need to coat samples, and should make it possible to observe fine scale topography as well as utilising potential contrast effects of secondary emission dependent on crystal structure, orientation and to a more limited extent on surface chemistry.

No major development of components is required : the existing technology should be entirely adequate and the only innovations are in the way in which the components are used.

The essential features of the new instrument are the combination of a high brightness and low energy spread field emission gun (FEG) operating at up to 15kV with a high quality lens and stage system in a very short, mechanically rigid and magnetically well screened column. Inadvertant coating of the specimens will be controlled by providing a clean ion pumped vacuum system equipped with a cryobaffle and an airlock.

The differentially pumped gun chamber will be fully UHV ($1x10^{-10}$ torr).

The test rig is intended to establish the conditions for LVSEM and to perform comparably with the best conventional SEMs i.e. 5-10nm resolution. In principle it should be possible to achieve substantially higher resolution, under appropriate conditions.

There are possible applications to more general improvements in the resolution of surface topography; to very high resolution microanalysis of bulk samples and of extensions to even lower voltages (<1kV) where there are new contrast modes to be exploited.

****

Some of the basic information on the LVSEM project, design aspects of the instrument, and collected physical data relating to operation of an SEM at low voltages; was included in the second annual report on this project (June 1985) to which readers of this report are referred for additional information.

****

4. SCIENTIFIC PROGRAM

There have been two parts to the project. In addition to the design and construction program for the novel LVSEM instrument, there have been a series of calculations and experiments to refine the potential of the low voltage scanning electron microscopy technique. The results either have been published, or soon will be, of calculations to define the potential optical performance of future LVSEM designs and of exploratory imaging and microanalysis caculations and experiments at low voltage and at low impact parameters (using higher voltage beams at high angle of tilt to reduce the energy component normal to the surface).

(a) Applications to x-ray microanalysis

The essential problem leading to the specification of a LVSEM is illustrated (Fig.1), for a conventional microprobe operated with 20nA probe current, by the contrast of the alumunium (K) x-ray signal as the probe is scanned over a 1.3μm wide band of pure gallium arsenide (GaAs) sandwiched between 5.6μm wide layers of gallium-aluminium-arsenide (GaAlAs) in a fabricated multilayer structure. At voltages >15kV the x-ray linescan resolution is dominated by the range of the electron beam in the sample, but below ~10kV the resolution and contrast of the GaAs band is reduced by the expanded probe size as the voltage is reduced. The most accurate analysis of this heterogeneous structure is obtained under the same conditions for maximum contrast of the band. More sensitive x-ray detection, and smaller probe currents, would move the crossover point between the specimen dominated and instrumental limits on the resolution to somewhat lower voltages; but the general picture continues to have a similar form.

A minimum voltage $W.E_x$ - typically W>1.7x the x-ray line energy (E_x) - is required to generate a signal with reasonable efficiency. The advent of efficient windowless energy dispersive (EDX) x-ray detectors with good sensitivity at E_x <<1keV (Fig.2) and able to detect a useful boron signal at 190eV (0.19keV) opens up new possibilities of using low energy signals from the K lines of the light elements- particularly C,N,O - and the L and M lines of heavier elements with beam energies of 1kV or less. General application is inhibited by the broad peak overlap in the low enegry regime with full width half maxima of typically 80eV, but this does not preclude more controlled applications, eg with semiconductor materials.

(b) Depth/Range experiments.

With a standard SEM, pending completion of the more specialised LVSEM, the limiting factor on the resolution of analysis is the rather large probe size that can be achieved at low voltages. It was shown in the previous section of this report that the resolution of analysis continued to improve down to a limit of ~0.3μm set by the probe size attainable with the particular instrument and conditions being used. A further limitation may be the minimum voltage required to excite a specific signal with sufficient efficiency for an acceptable signal to noise (S/N) at a given probe current.

Two sets of experiments have been performed to examine the potential for improved resolution at low voltage [this work will be published in 1989, as indicated in the summary of this report]. Since at low voltage the lateral resolution of the experioment is limited by the probe size of the available instrumentation; the depth sensitivity of the signal has been examined with specially fabricated specimens in an on-going series of experiments. The assumption from available theories, and on the basis of published Monte Carlo trajectory simulations, is that the interaction volume approximates (hemi)spherical symmetry with similar depth and lateral components (Fig.3). On this basis we have examined the total range of electrons from a beam with initial energy E_o, predicted by the various models, and have started to measure the practical range for x-ray microanalysis; with a view to using the measured vertical, or depth, sensitivity of the signal to estimate the lateral spatial resolution that might be achieved; if the present severe limitations of the electronoptics of existing (conventional) SEMs were improved substantially in a developed LVSEM instrument.

The original Bethe continuous energy loss equations describe the trajectory of electrons along a pathlength as a function of the sum of all energy loss processes. The energy loss per unit distance travelled in the solid, dE/dx, is given by :-

$$dE/dx = -2\pi e^4 N_o (Z_\rho/AE_m) \ln(1.66E_m/J)$$

$$= -7.85\times10^4 (Z_\rho/AE_m) \ln(1.66E/J) \text{ keV/cm}$$

where e is the electronic charge,
N_o is Avagadro's number,

Z is the atomic number,
A is the atomic weight (g/mol),
ρ is the density (g/cm^3),
E_m is mean electron energy (keV) along the path,

and J is the mean ionisation potential (keV), given by :-

$$J = (9.76Z + 58.5Z^{-0.19})10^{-3} \quad keV$$

The total distance travelled by an 'average' electron is given by :-

$$R = \int_{E=E_o}^{E=0} \frac{1}{dE/dx} \, dE$$

and when the Bethe formula can be used to get the Bethe mass range, $\rho.R_B$ (g/cm^2) :-

$$= \int_{E=E_o}^{E=0} \frac{1}{(dE/dx).(1/\rho)} \, dE$$

By definition (Fig. 4) the Bethe range distance is somewhat longer than the outer envelope of the interaction volume within which the electron paths lie in the solid sample, and Kanaya and Okayama (J Phys D Appl Phys 5 (1972) 43) have derived an expression for the radius of a hemispherical interaction volume centred on the point at which the probes incident on the surface of the specimen :-

$$R_{KO} = 0.0276AE_o^{1.67}/Z^{0.889}\rho \ \mu m$$

where E_o is the beam energy in kV,
A is the atomic number in g/mol,
ρ is the density in g/cm^3, and
Z is the mean atomic number of the target.

The data (in μm) for Aluminium (Z =13) are summarised as follows:

	2.5kV	5kV	10kV	20kV	30kV
Bethe R =	0.18	0.56	1.80	6.04	12.4
K-O range =	0.13	0.41	1.32	4.2	8.3

For Gold (Z =79) the data are :

Bethe R =	0.06	0.20	0.55	1.63	3.18
K-O range =	0.03	0.09	0.27	0.86	1.70

The practical application was examined with a deposit of 55nm of aluminium (Z = 13) on the flat surface of a silicon (Z = 14) single crystal at normal incidence in a conventional SEM equipped with an EDX analysis system.

The spectra recorded with a high energy beam - the 25kV data in Fig.5 is typical - were dominated by the signal from the substrate into which the beam penetrated through the thin film. In these data the 55nm thick aluminium film was only a small fraction of the total excitation volume in the sample, due to the long penetration (range) into the substrate. However at 5kV the Al and Si peak heights were similar and we deduce that the penetration depth from which x-rays were being generated was approximately twice the film thickness.

At 2.5kV only the Al signal is present suggesting that the range for generating the x-ray signal is <55nm. This is substantially less than the K-O range predicted from the above equations and included in the data chart.

Consideration of the basis of the two approaches suggest that the two results can be reconciled by considering the origin of them. The K-O etc expressions describe the total electron range within the sample, but only those electrons with an energy $E>>E_x$, ie $W>>1$, are effective in exciting x-rays. When the beam energy (E_o) approaches E_x the rate of production of x-rays is rapidly reduced. The range for effective x-ray production is therefore the integral between E_o and $W.E_x$ ($W>1$), rather than the calculation between E_o and $E = 0$ used for the total range. In the past the total

range measurements have been made on samples through which electron transmission could still be obtained. To use the same equations for calculating an x-ray analysis range is conceptually unsatisfactory, but has been the conventional practice over many years. One can surmise that the errors will become appreciable only as E_o approaches $W.E_x$, with $1<W<3$; which is the condition we are exploring at lower voltages. For example the correction for the 1.47keV Al(K) line at 25kV ($W = 17$) is expected to be small; but to become more significant as E_o is reduced and $W \rightarrow 1$. There should be a sharper dependence of the radius of the excitation volume as $E_o \rightarrow E_x$, and this is what we observe experimentally. At low voltage the penetration depth is smaller than predicted by the total range equations (Bethe, K-O etc).

(c) Calculations of predicted LVSEM resolution and associated instrumental design requirements

The potential of low voltage imaging depends on the optical performance that can be achieved. Fig. 6 is an extension of the results presented at the Kyoto meeting in 1986 (see appendix for reprints of published papers), based on the prediction that lens parameters as low as $Cs = 0.15mm$ and $Cc = 0.4mm$ could be achieved in the enhanced second zone mode of operation. The bases of these estimates are (a) finite element lens calculations (Munro, Cambridge University Engineering Laboratory, 1975) and (b) the application of this data in our standard calculation of SEM probe size (with $A = 1$) performance on the basis of the following equation :-

where

Cs and Cc, are respectively the spherical and chromatic aberration coefficients of the final lens
α, is the probe semi-angle in steradians (Sr),
β, is the effective source brightness ,in units of ($Amps/cm^2/Sr/volt$),
V and ΔV are the accelerating voltage and the energy spread of the beam, and
λ is the electron wavelength corresponding to V.

Probe currents of $1x10^{-11}$Amps (10pA) and 1pA, corresponding to conditions often used for high

resolution recording of images from good contrast specimens at high voltage, were used in the calculations. Typical results are reported in Fig.6. It has been claimed (eg Venables et al) that the the edge resolution of an SEM image, as measured by the 10% - 90% risetime over an edge, can be better than the probe size determined point resolution (A = 1) by up to ~3x, depending on the probe current and its distribution. These values are also of interest as an accepted SEM resolution test method.

Each of the terms in the above equation has a dependence on both the accelerating voltage (V) and the aperture semi-angle (α); as well as on the basic (eg lens) parameters of the microscope. Of course, at low voltage it is desirable to be able to select V independently to optimise the interaction with the specimen; appropriate to the chosen imaging signal. The current is maximised by choosing the largest aperture consistent with acceptable geometrical aberrations of the probe for a given magnification (a resolution of 1nm is only required at the magnifications >200,000x at which it is visible).

At high voltages (>20kV) the spherical aberration dominates the high resolution performance of an SEM but as the voltage is reduced the chromatic and brightness terms become increasingly important.

We conclude that with an appropriately advanced lens design, but one still based on existing technology, (curve #L2, corresponding to Cs = 0.27mm, in Fig.1) it should be possible to approach a probe size of <2nm and an SEM image resolution of 1nm or less at 1kV.

(d) <u>An investigation of specimen tilt effects</u>.

Data collected from the literature on the yield of secondary electrons from various materials is plotted within the envelope in Fig.7. The total electron yield is made up of the (SEI) secondary (δ) and (BSE) backscattered electron (η) components (as well as some absorption (I_a) of the probe current, I_p).

To avoid charging it is necessary for :

$$Ip = I.\delta + I.\eta + I.a$$

It is clear from Fig.7 that over much of the typical SEM operating range $\delta << 1$. The BSE yield (η) depends on

the atomic number (Z), according to the standard equation :

$$\eta = -0.0254 + 0.016Z - 1.86\times10^{-4}Z^2 + 8.3\times10^{-7}Z^3$$

with a value of $\eta = 0.06$ for carbon ($Z = 6$) and $\eta = 0.30$ for copper ($Z = 29$) and $\eta = 0.50$ for gold ($Z = 79$). For most elements $\eta < 0.5$; and for many of them $\eta << 0.5$.

At high voltages the yield of secondary electrons is also and there is charging of uncoated non-conducting samples (for which $I_s = 0$). However as the specimen is tilted with respect to the beam, the yield of both backscattered and secondary electrons increases and charging effects may be reduced. It should be noted that the relationship between the yield of electrons from a sample and the collected signal will depend on the detection system being used.

In Fig.8 the results of calculations for the BSE and seconadary yields for iron, as a representative mid-Z element, are plotted as a function of tilt angle (θ), on the basis of :

$$\eta(\theta) = 1/(1 + \cos\theta)^p, \text{ where } p = 9/Z^{1/2}$$

and

$$\delta(\theta) = \delta o.\sec\theta$$

At higher angles of tilt ($\theta > 45°$), both yields increase by significant amounts. At a tilt angle of $\theta = 76°$ the total yield is unity ($\delta + \eta = 1$) for secondary and backscattered electrons, the absorbed current requirement is predicted to fall to zero and charging of non-conducting samples should be avoided. Of course in practice a tilt angle of 76° is very high. There are the general problems of focus correction and image foreshortening with high tilts. In many instruments the use of very high angles of tilt are limited to small specimens.

It should be noted that the effect is limited to those parts of a specimen which are at an appropriate angle of tilt and other parts could charge up as before. However there may be specialised applications, for example to the examination of coatings on optical surfaces; or for microcircuit substrates.

Tilt has also been used constructively to extend the

control of the impact parameter and hence the depth from which the signal is generated. Since a certain beam energy ($E_o > W.E_x$) is required to excite characteristic x-ray lines with an energy E_x, and there are limitations in running a conventional SEM at very low energies, the range of useful application can be expanded and the surface sensitivity of analysis can be improved by the controlled addition of tilt. The comparison is illustrated in Fig.9, which has been published previously as referenced in the appendix to this report.

It will be seen that with normal incidence and a 20kV beam, the Au(M) signal is very small from the ~10nm thick gold film on the surface of the silicon substrate. At 5kV the gold signal is proportionately much greater, and can now be used for analysis. At high angle of tilt ($\theta = 84°$) the Au(M) peak is now the largest one in the spectrum. The absolute height of the Au(M) peak is similar to that at normal incidence, but the Si(K) signal from the substrate, which has a similar energy, has been reduced substantially (even though there is evidence that the gold film is not uniform in thickness or coverage).

A series of experiments is planned to explore more fully the potential for improved imaging and enhanced EDX x-ray microanalysis at low voltage and/or high angles of tilt, on the basis of the preliminary data presented in this report.

5. Progress in constructing the specialised LVSEM instrument.

The design of the instrument has been covered in outline in the initial proposal to the US Army, and more comprehensively in the subsequent reports. There have been only minor modifications in the implimentation since then. The basic diagram of the instrumented is repeated as figure 10 to summarise the design etc and to aid in interpreting the photographs of the column and console (figs.11-13). Completion of the instrument to full operation has been delayed by a number of problems associated with a faulty connection in the control electronics for the vacuum pumping system, which was only diagnosed with the aid of an additional turbomolecular pump provided from departmental resources to evacuate the airlock efficiently. Since this was done, a vacuum of <1x10-7 torr has been consistently achieved in the specimen chamber; even without baking the machine. THis is better than expected, but we now think it should be improved further. Time has been lost due to the need to dismantle parts of the column to get access to the vacuum flanges. It will be seen that

adapters have been made for some of the ports, including the aperture, to reduce the extent of this problem. We also customarily leave off the outer magnetic screening tube to improve access. The additional screening may be needed in later operations. A revised UHV specimen chamber would be designed with conventional UHV flanges; which should prove more reliable than the present viton o-ring seals, and would be made accessible from the outside of the column without the need to remove screening to minimise the dismantling required to make even minor changes to the configuration and for improved access for diagnosis and servicing etc. The scan coils have been installed and the scanning electronics have been completed for scanning at TV rate and with an AC mains synchronised slow scan (analogue line scan and digital frame at this time). Only TV displays are provided and scan conversion is needed to display the slow scan signal. The arrangements for shared use of a digital framestore for this purpose have not been very successful due primarily to the demands this has made on an existing, and not very reliable framestore system. Useful progress will depend on being able to get a dedicated framestore for the machine (at a mimimum cost of $18,000).

We need to complete testing of the scanning system, to install a revised secondary electron detector, to fully bake the column and to changeover from the thermionic gun control electronics to those designed and built to operate the field emission gun. The latter will probably need some refinement; with a discrete 0-5kV or 0-7kV EHT module to replace the adapted 0.1 to 30kV EHT set presently being used.

The general conclusion is that the goals of the project were scientifically correct, even from the initial inception. However the resources available, and particularly the heavily cut back capital provisions, were inadequate to complete the project within the time frame of the existing contract. Comlpetion of the project will depend on being able to redirect some of the remaining resources to increase the capital account.

6. STATUS OF LOW VOLTAGE SCANNING ELECTRON MICROSCOPY

Low voltage (1-4kV) operation of standard SEMs has become routine in the semiconductor industry. It is used to test devices, using the voltage contrast signal, and for inspecting CMOS devices; in addition to the established use for design verification and the analysis of manufacturing defects. The ~0.1μm image resolution of a regular SEM at ~1kV has not yet been a serious

limitation for these applications; but improved microscope electronics, and vacuum system quality, have been necessary. In polymer science, where there have also been significant applications, the superior resolution attainable at low voltages with a field emission gun is important.

It has been established that the goals of the LVSEM project were essentially correct. There are indeed major advantages of image contrast, and reduced charging of electrically non-conducting samples, by operating the SEM with a low voltage electron beam. The resolution and probe current are both reduced at lower voltages. With a regular SEM these effects are especially pronounced below 5kV, where the chromatic abberation terms become dominant and the gun performance is compromised by the need to also provide for operation at high voltages (>20kV). As pointed out in the original proposal, two major improvements are possible. Firstly, a field emission electron gun (FEG) with a much higher brightness (~1000x) and significantly lower energy spread can replace the conventional tungsten or lanthanum hexaboride source. Secondly, the final lens optics, and abberations, of a regular SEM can be improved, from typical values of Cs = 75mm and Cc =20mm, by using a TEM-style condenser-objective lens with Cs and Cc <5mm. In this type of lens the specimen is immersed in the peak field of the lens and is limited in thickness to a few, typically 1-2, millimeters. A TEM side entry stage also provides the superior stability which may be required to improve the practical image resolution.

The LVSEM proposal was to combine both these approaches in a new type of instrument, designed specifically for operation at low voltages in the range 0.5-5kV; with a limited higher voltage capability for analysing image contrast in the same instrument. It was shown during the development of the project, and published in 1986, that substantially better lens abberations, with Cs = 0.15mm and Cc = 0.4mm, could be achieved for an SEM at low voltage than for a TEM at high voltages (>100kV). The lens excitation and peak field (>1T) are comparable to those often used for TEMs, but the specimen is moved up towards the entrance polepiece and the lens is operated in a new, and extreme, multiple zone mode; based on Kaminga's (Optik ,45 (1976) 39) second zone model.

A number of laboratories in Japan (Tottori) and the USA (Yale and Wisconsin) have used field emission gun SEMs to initiate higher resolution imaging studies, almost entirely of biological material. The samples have continued to be metal coated : to limit charging and to

improve the nanometer-scale high resolution image contrast for operation at higher voltages (~30kV at Yale), or to enhance the lower voltage signal, at more modest resolution (at Wisconsin). Substantial improvements in the control of coating deposition, down to the nanometer level, have been achieved in these programs.

A commercial high resolution (<1nm at 30kV) field gun SEM became available from Hitachi in 1986-7, and it has been used to initiate high resolution programs with a strong low voltage component at the Universities of Tottori, who collaborated in the design, Wisconsin and Tennessee. The instrument is reported to be able to achieve a secondary electron image resolution of 4nm at 1kV, with a probe size <<10nm. Most applications to date seem to have explored the high voltage, ultra-high resolution capability of the instrument. The lens parameters of the Hitachi instrument (Cs = 1.9mm and Cc = 2.6mm) are not as good as our own design with Cs and Cc <1mm, but it clearly demonstrates that the big improvement in specification over a standard SEM translates into superior low voltage performance.

On the basis of the calculations done in the LVSEM project it was predicted that it should be possible to achieve an image resolution of ~2nm at 1kV. This is now more widely accepted as a realistic goal for LVSEM. Improved lens parameters are a necessary component of this progress, but whether other changes will also be necessary is unclear at this time. Efficient collection of the low energy (typically 0-10 eV) secondary electron signal in the presence of the low voltage (~1kV) primary beam is a serious problem on all of the instruments used at low voltage. We would like to extend the range of operation below 1kV, where there are new contrast modes to be explored and contamination damage may be reduced substantially, but this will almost certainly required a different - and more symmetrical - detector design. With the present assymetrical design, including on the LVSEM, collection efficiency is sacrificed to limit probe deflection by the detector accelerating field. In principle, an annular design, possibly based on microchannel plates, should reduce this problem. The LVSEM achieves part of this design goal with an extraction field at an acute angle to the incident beam direction, ie with a substantial vertical component. The effect should be some readily compensated defocussing action and a reduced deflection, and hence abberation, of the primary beam.

The secondary electron image contrast mechanism at low voltage has been considered, primarily by Professor Joy at the University of Tennessee. As might be expected at

this stage, the conclusions are still somewhat incomplete; and the experimental evidence is limited. However he has identified a number of factors which will need to be considered explicitly. Firstly the shape of the low voltage probe will have a substantial 'tail', much wider than the main intensity peak, and this problem will get worse as the voltage is reduced. Secondly the contribution to the image contrast from backscattered electrons will be mopre intense at low voltage, where the range and spread of the beam-specimen interaction will be greatly reduced. Usually this is seen as an advantage, but Professor Joy's calculations clearly show that the component of the high resolution secondary electron signal arising from primary backscattered electrons will be much more significant, at least down to 2kV. At very low voltages in the range 0.5-1kV the problem may be reduced by an interaction range which is extremely short and comparable to the enlarged probe size under these conditions. The general conclusion may be to operate either at high voltages >20kV, or low ones <2kV and avoid the complexities of the intermediate voltage range.

The potential applications of backscattered (BSE) imaging have yet to be explored at low voltage. They provide the potential for very high resolution chemical microanalysis, although some data from Reimer's group suggests a a modified, and voltage dependent, form of the atomic number dependence at voltges below 5kV. A resolution of 0.1μm has been demonstrated at 30kV, and in principle it should be possible to do very much better, possibly <0.01μm (10nm) at low voltages. It will be necessary to design efficient BSE detectors, compatible with the geometry of low voltage lenses in order to achieve this. Substantial progress with the BSE technique can probably be made at intermediate voltages of 3-10 kV in a regular SEM, or one fitted with an FEG.

7. FUTURE DIRECTION OF LVSEM

Now that low voltage technique is firmly established and the first phase of the LVSEM program is being concluded, it is appropriate to consider the developments which are needed in the basic instrument and for specific applications.

1. It should be possible to improve the low voltage SEM instrument to achieve an image resolution of 1-2nm at

1kV, by using better optics, along the lines of our 1986 paper.

2. Improvements are needed in the collection efficiency of the secondary electron detector, consistent with avoiding introducing additional electron optical abberations due to off-axis electrostatic field components.

3. The ability to operate for the first time with uncoated ceramic substrates permits in-situ deposition studies related to ceramic-metal bonding and catalysis applications.

4. There would be major advantages in having an ultra high vacuum (UHV) specimen environment, in the 10^{-10} torr range.

5. Heating and cooling specimen stages.

6. With the LVSEM there is the potential to improve substantially the spatial resolution of x-ray microanalysis of bulk SEM samples and thin films (see paper #). With a conventional microprobe the lateral and depth resolution is typically 1μm or more. Using lower energy x-ray lines allows the the beam voltage to be reduced by a corresponding amount. The energy dependence of the resolution is usually taken to follow a $E^{1.7}$ power law. A detailed series of measurements on the depth dependence as a function of voltage is in progress and the results will form part of an LVSEM paper which the author has been invited to present at SEM West meeting in San Diego in April 1989. It will be contended that depth, which can be measured with excellent accuracy, has a similar dependence to the lateral resolution which is also of interest in many applications. However the depth model is important for analysing reliably thin film on substrate samples.

7. X-ray microanalysis could be extended to voltages below 2kV by specifying a windowless energy dispersive x-ray detector, of the type used to obtain the spectrum in figure # of paper #. The potential improvement in resolution from using 2kV beam and the CuL lines instead of a 20kV beam and the CuK lines, is approximately 50x. Conventional wisdom, on the basis of the KO relationship, suggests the resolution would be ~0.03μm (30nm) at 2kV, compared to ~1.5μm at 20kV. The very short path length in the material, should minimise absorption of the x-rays in the sample. The low energy x-ray lines have not been widely used for quantitative microanalysis until now due to poor detection efficiency, inadequate cross-section data and concerns

about the extent of absorption with the >1μm pathlength typical of high beam energies. The new type of windowless x-ray detector used to produce fig. in paper # takes care of the detection efficiency; the low energy LVSEM beam reduces the absorption problem to manageable proportions, and for specific situations, appropriate standards should cope with the limited reliability of the L and M line cross-section data.

8. The high resolution capability of the new type of SEM should allow many more projects with bulk samples. These have major advantages, compared to TEM thin foils, of stability and wide area scanning in a complex microstructure. The relative ease of producing representative samples for the SEM may be particularly important for interface cross-sections.

We envisage a developed LVSEM with an improved image resolution at low voltage and an extended high voltage range of 0.5-30kV. It would have an integral digital imaging system, a UHV specimen environment, a heating stage and a UHV compatible windowless EDX detector for chemical microanalysis.

8. SPECIFIC RECOMMENDATIONS

(a) The US Army should recognise the scope and importance of operating conventional SEMs at low voltage and should include this as an operating requirement for all new SEMs purchased for its laboratories.

(b) The advantages of low voltage operation should be publicised and encouraged.

(c) Specific intiatives identified in this report, including microanalysis of thin films at low voltage, should be followed up.

(d) The potential advantages of a dedicated high resolution and/or ultra high vacuum LVSEM should be recognised.

(e) The Oxford Department should be encouraged to complete the LVSEM to functional status and eventually to make it available for further evaluation of the technique by the US Army and the sponsoring laboratories.

9. List of Illustrations

Fig.1 : Image contrast as a function of beam energy. At high voltages the limit is set by the range of the beam/specimen interaction, and at low voltages by the condition dependent probe size of the instrument.

Fig.2 : X-ray spectrum recorded at 100kV using a windowless energy dispersive (EDX) detector with sensitivity extending to the light elements (C,N,O etc; O in a high Tc superconducting oxide ceramic ($YBa_2Cu_3O_{7-x}$) is illustrated), and to the low energy lines of heavier elements (eg the Cu(L) peak at 0.91keV and of similar height to the Cu(K) peak at 8.04keV).

Fig.3 : Hemispherical model of the x-ray source/electron interaction volume (after Kanaya and Okayama [K-O]), with the different radii appropriate for x-ray lines of different energy, corresponding to the range before too much energy is lost for the beam to continue to excite the specific x-ray line ($E = W.E_x$; $W = 1.7$ and $E < E_o$) for a given value of E_o.

Fig.4 : Definitions of Bethe and K-O ranges.

Fig.5 : New EDX data from a specimen with a 55nm thick (t) Aluminium film deposited onto a flat Silicon substrate. Beam at normal incidence (90°). At a high beam energy (E_o=25kV) the radius of the interaction volume (R_x), the depth from which the x-ray signal is being generated in the specimen (see Figs.3&4) is very much greater than the film thickness ($R_x >> t$) and the x-ray spectrum (a) is dominated by the Si(K) x-ray signal from the substrate. At 5kV the interaction volume has contracted until $R_x \sim 2t$ and the substrate (Si) and surface film (Al) signals are of comparable amplitude. At low voltage (2.5kV) the spectrum contains only the Al peak from the film, suggesting that $R_x < t$. The complete voltage sequence, from which only selected examples are shown here, confirms that this is a smooth progression. The K-lines of Al (1.49keV) and Si (1.74keV) are of comparable energy.

Fig.6 : LVSEM probe size and image resolution calculations.

Fig.7 : Literature values for the secondary electron yield as a function of incident beam voltage.

Fig.8 : Calculations of secondary electron and back-scattered electron yield for iron (Z = 26) as a function specimen tilt angle (away from normal incidence at $\theta = 0$).

Fig.9 : EDX x-ray microanalysis of ~10nm thin film of gold on a silicon substrate.

Fig.10 : General arrangement vertical cross-section diagram of main part of LVSEM column and vacuum lines.

Fig.11 : Side view photograph of the completed LVSEM column, corresponding to the diagram in Fig.10.

Fig.12 : Front of column with (a) the custom bellows sealed aperture mechanism, (b) the specimen airlock, (c) the airlock prepump valve (to TMP) and (d) the Y-stage drive (differential) micrometer. The gun alignment knobs and the high voltage cable connections to the gun (usually encased in a metal screening sleeve) are also visible.

Fig.13 : Overall view of microscope plinth with column and vacuum pumps. Separate ion-pumps at the top for the differentially pumped gun, with the specimen chamber ion pump and a turbomolecular pump for prepumping the microscope, and for routine evacuation of the specimen exchange airlock; located under the table.

Fig.14 : Main electronics console with display, control and vacuum electronics. The TMP controller is located under the microscope table (see Fig.13) and the electron gun supplies and controls are in the adjacent short electronics rack to the right of the main rack and visible in the bottom right hand corner of this picture. When the digital imaging system is available it is wheeled in and connected temporarily to this instrument (or to several others). The two boxes on top of the main rack are the ion pump controllers.

Fig.15 : "Engineering for Low Voltage SEM"

[Summary of LVSEM Specification (from a panel of the poster presented at 11th ICEM, Kyoto, Japan, 1986)]

Fig.16 : Image of defect in cement fracture sample imaged uncoated and without charging artefacts at 1kV. [Scale is 0.1mm].

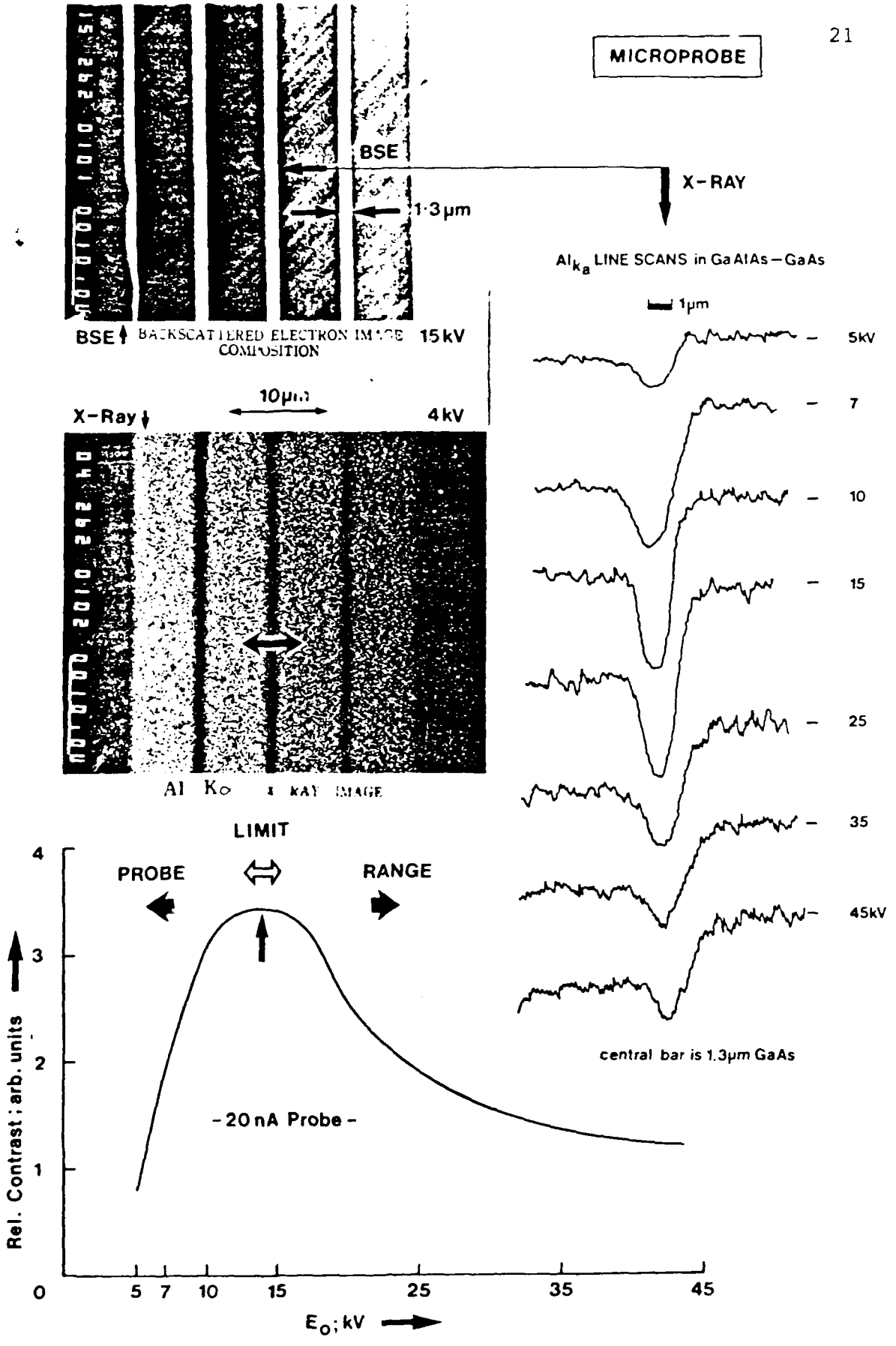

Fig.1 : Image contrast as a function of beam energy (E_o, kV). At high voltages the limit is set by the range of the beam/specimen interaction, and at low voltages by the condition dependent probe size of the instrument.

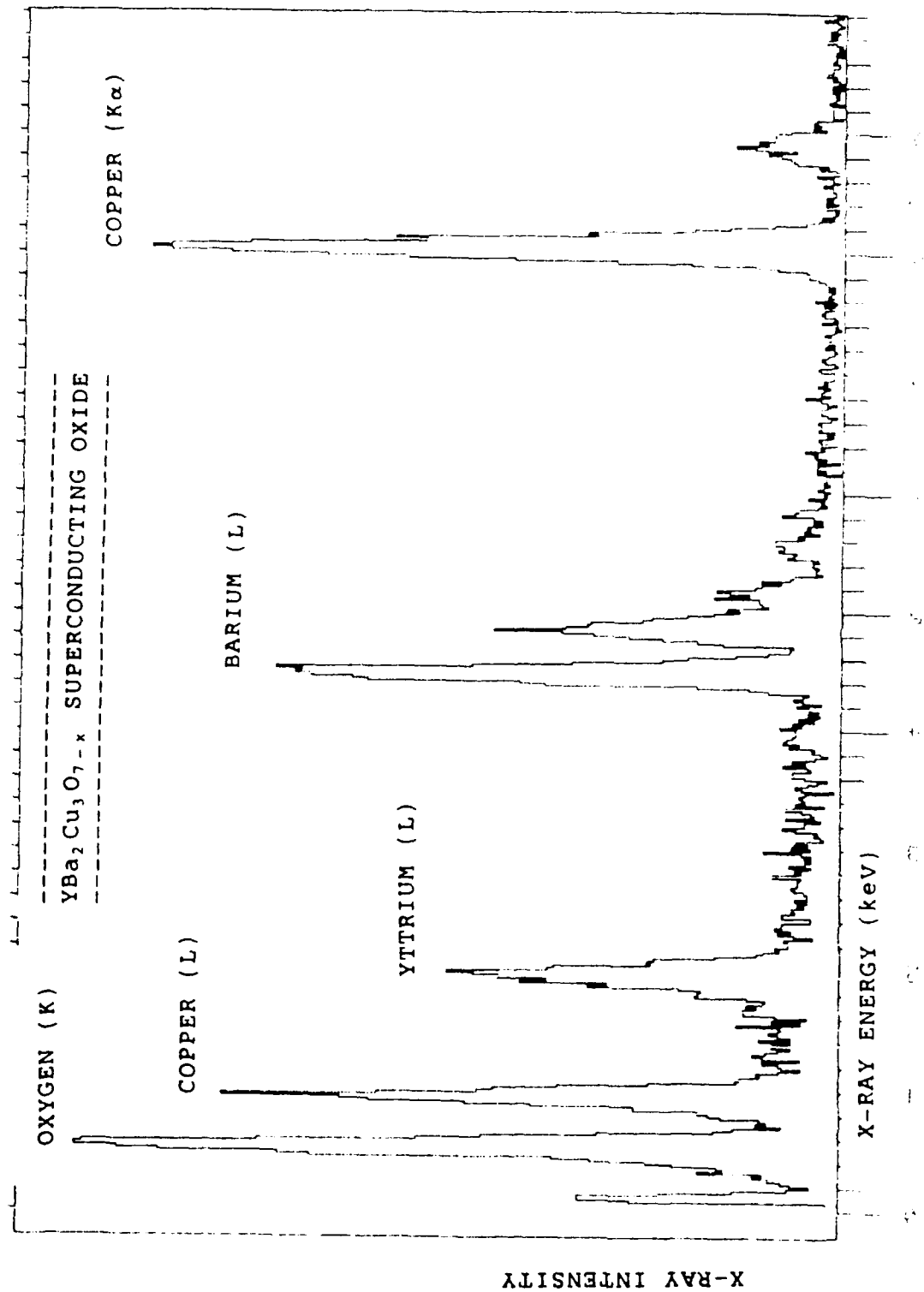

Fig.2 : X-ray spectrum recorded at 100kV using a windowless energy dispersive (EDX) detector with sensitivity extending to the light elements (C,N,O etc; O in a high Tc superconducting oxide ceramic ($YBa_2Cu_3O_{7-x}$) is illustrated), and to the low energy lines of heavier elements (eg the Cu(L) peak at 0.91keV and of similar height to the Cu(K) peak at 8.04keV).

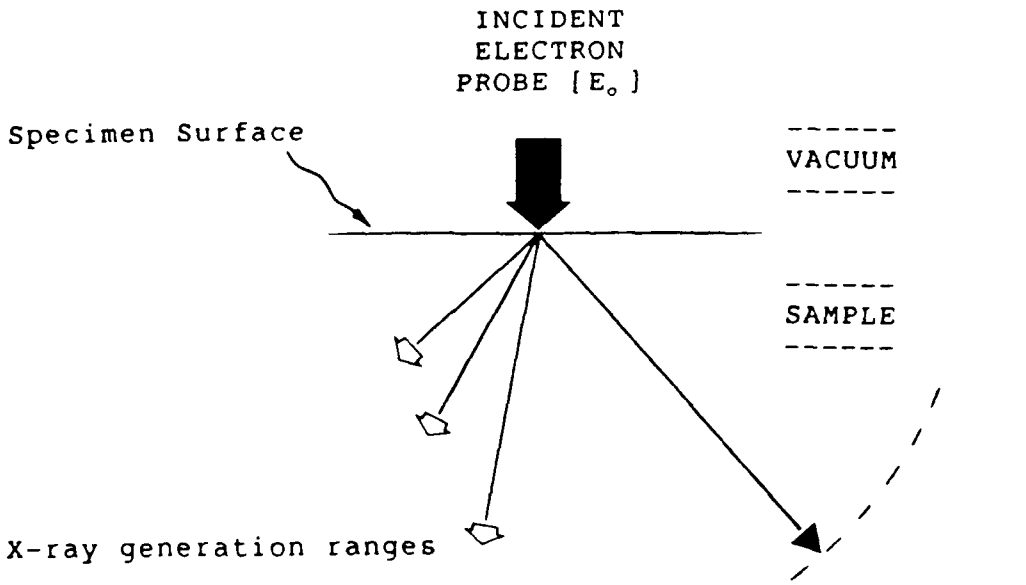

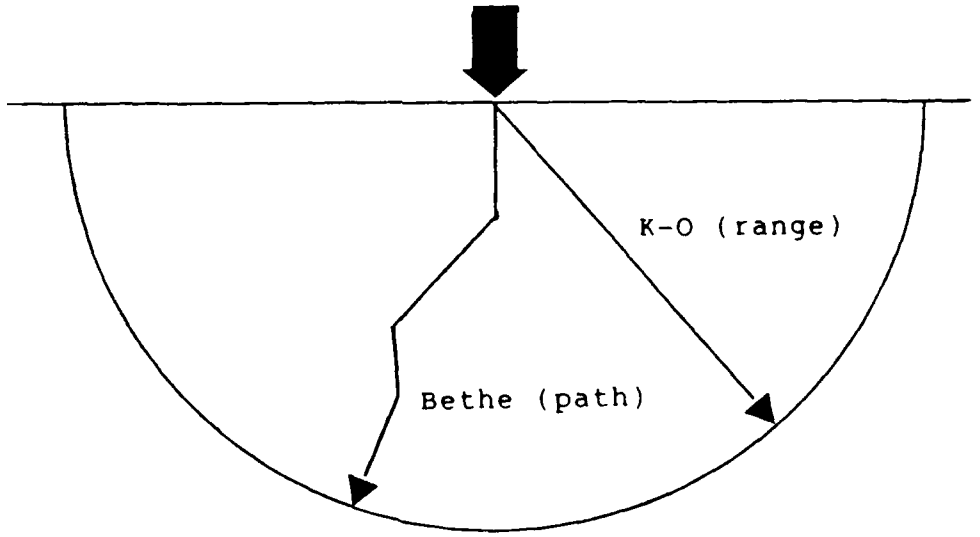

Fig.3 : Hemispherical model of the x-ray source/electron interaction volume (after Kanaya and Okayama [K-O]), with the different radii appropriate for x-ray lines of different energy, corresponding to the range before too much energy is lost for the beam to continue to excite the specific x-ray line ($E = W.E_x$; $W = 1.7$ and $E < E_o$) for a given value of E_o.

Fig.4 : Definitions of Bethe and K-O ranges.

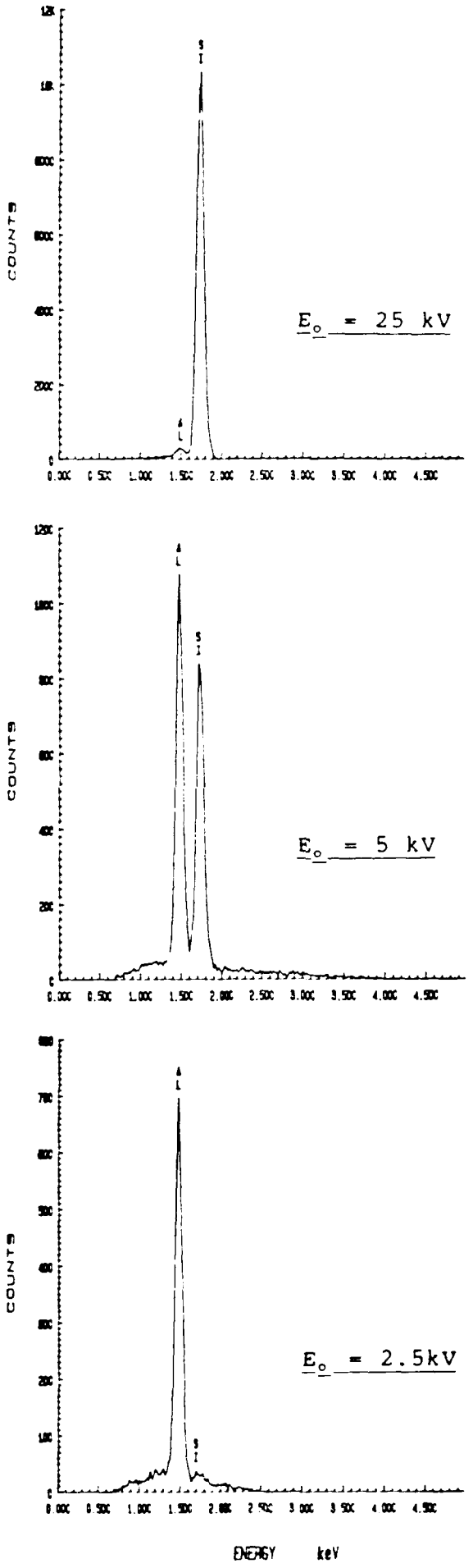

Fig.5 : New EDX data from a specimen with a 55nm thick (t) Aluminium film deposited onto a flat Silicon substrate. Beam at normal incidence (90°).

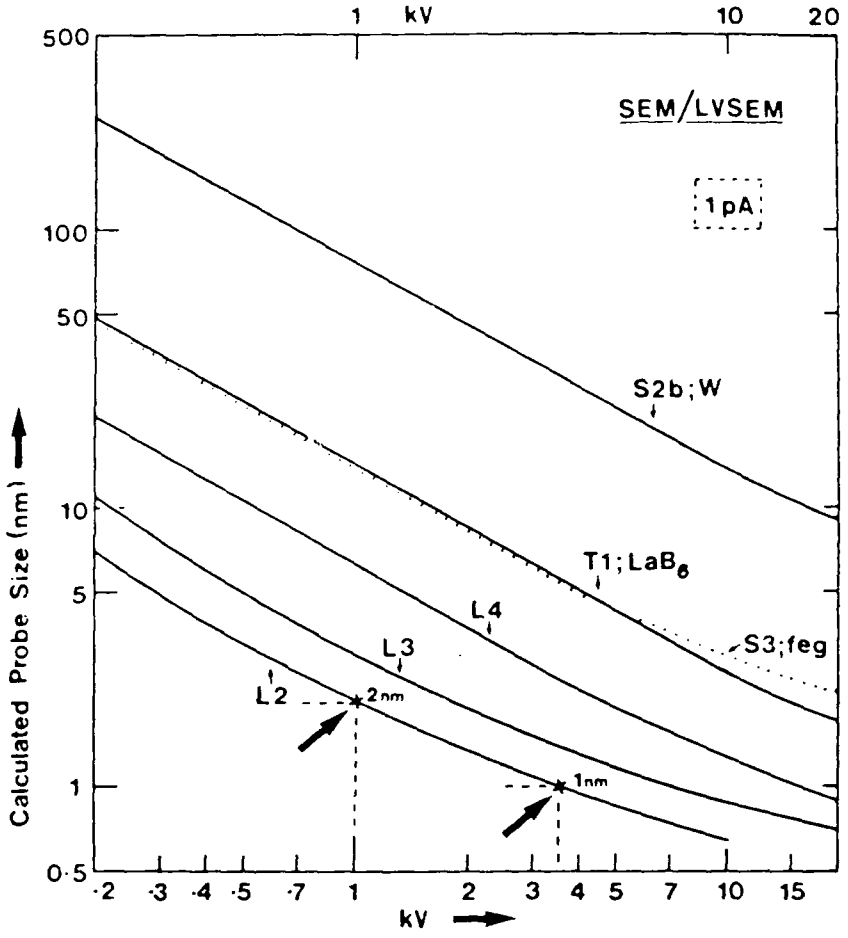

Fig.6 : LVSEM probe size calculations :

Fig.6 contd : For the following sets of parameters for standard SEMs and LVSEM specifications :

		C_s (mm)	C_c (mm)	β(A/cm²/Sr/V)	ΔV(eV,RMS)
S1:	Regular SEM	75	20	2/W	2·5
S2:	"	"		"	"
2B:	"	"		"	1·0 (2·4eV, FWHM)
S3:	FEG SEM	"		1000/FEG	0·2 (0·5eV, FWHM)
T1:	TEM/SEM	2·0	2·0	20/LaB_6	1·0
L1:	LVSEM 1	1·0	1·0	1000/FEG	0·2
1B:	"	"		"	0·5
L2:	" 2	0·27	0·4	"	0·2
L3:	" 3	1·0	1·0	"	"
L4:	" 4	0·27	0·4	20/LaB_6	1·0

Beam current (I_b) = 1×10^{-12} A (1pA) except S1 (I_b = 10pA)

(with A = 1), based on the standard equation :

$$d = A\sqrt{\left[\frac{4i}{\beta V.\pi^2\alpha^2} + (\tfrac{1}{2}.C_s\alpha^3)^2 + (C_c\frac{\Delta V}{V}\alpha)^2 + (\frac{0.61\lambda}{\alpha})^2\right]}$$

or

$$d = A\sqrt{(B + S^2 + C^2 + D^2)}$$

Predicted image <u>resolution</u> (nm) at 1kV :

		<u>S2</u>	<u>S3/T1</u>	<u>L4</u>	<u>L3</u>	<u>L2</u>
A = 1	:	76	18	6.3	3	2
(A = 0.3	:	23	5.4	1.9	0.9	0.6)

Low Voltage Electron Emission (BSE + SEI)
- at Normal Incidence on Flat Specimen.

Charging is avoided at E(0) = E(1), E(2);
and largely when E(1) < E(0) < E(2).

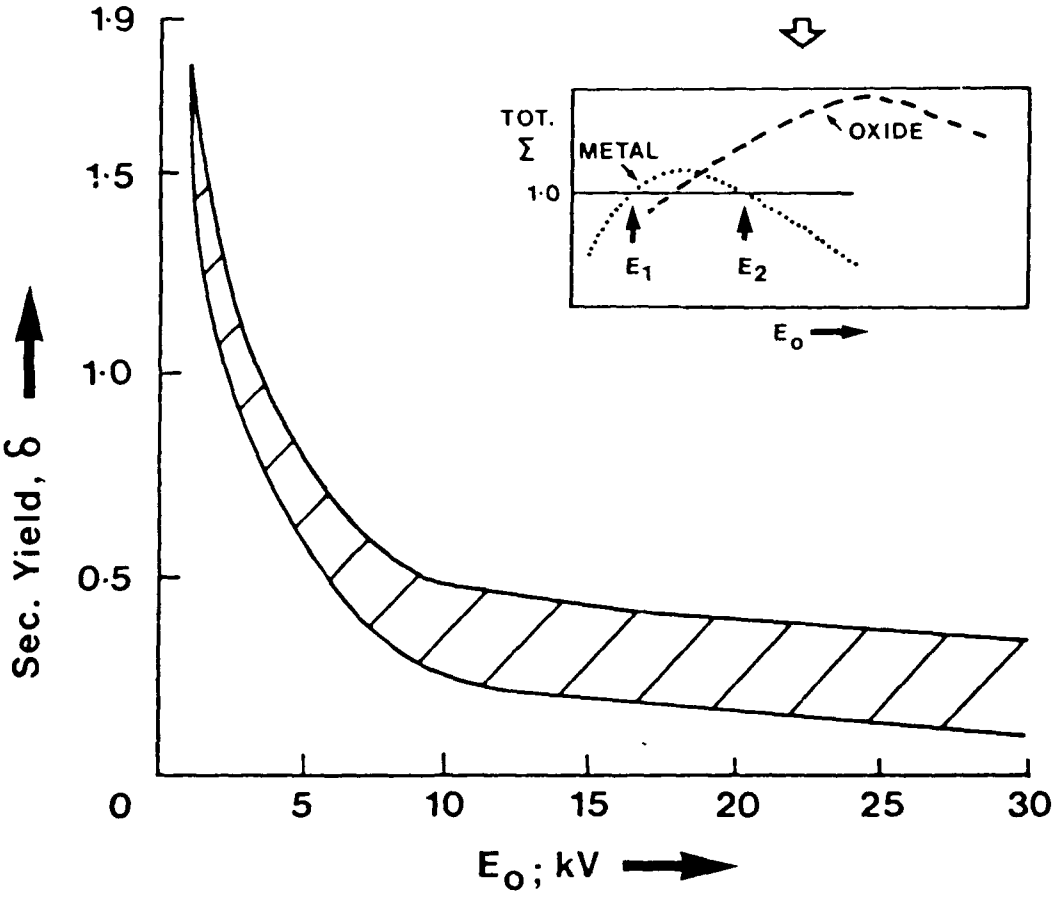

Fig.7 : Literature values for the secondary electron yield as a function of incident beam voltage.

Effect of TILT θ

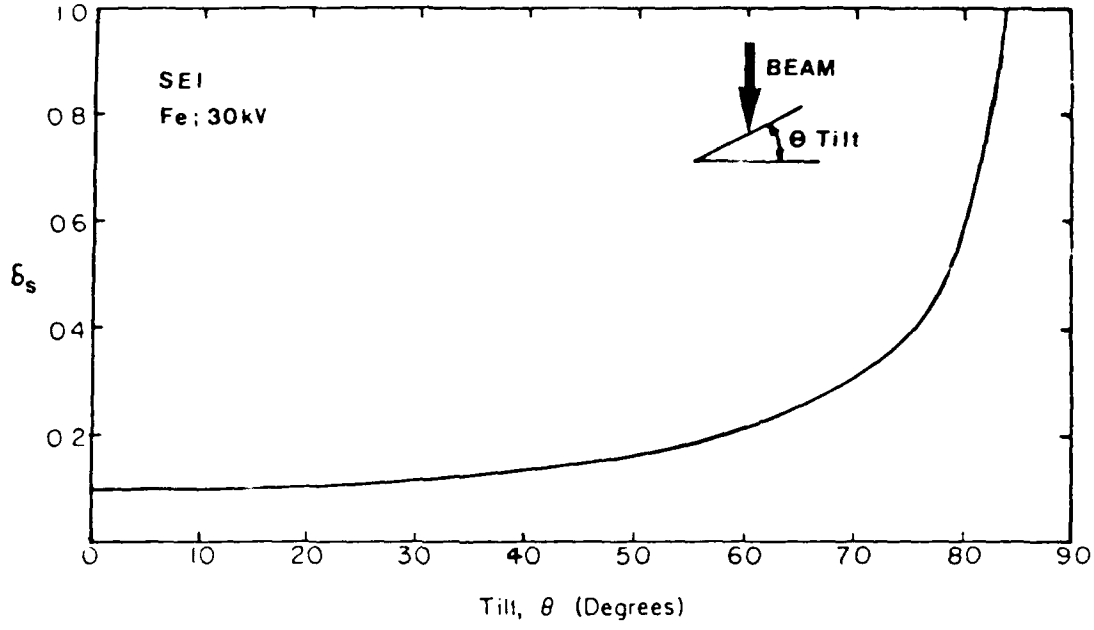

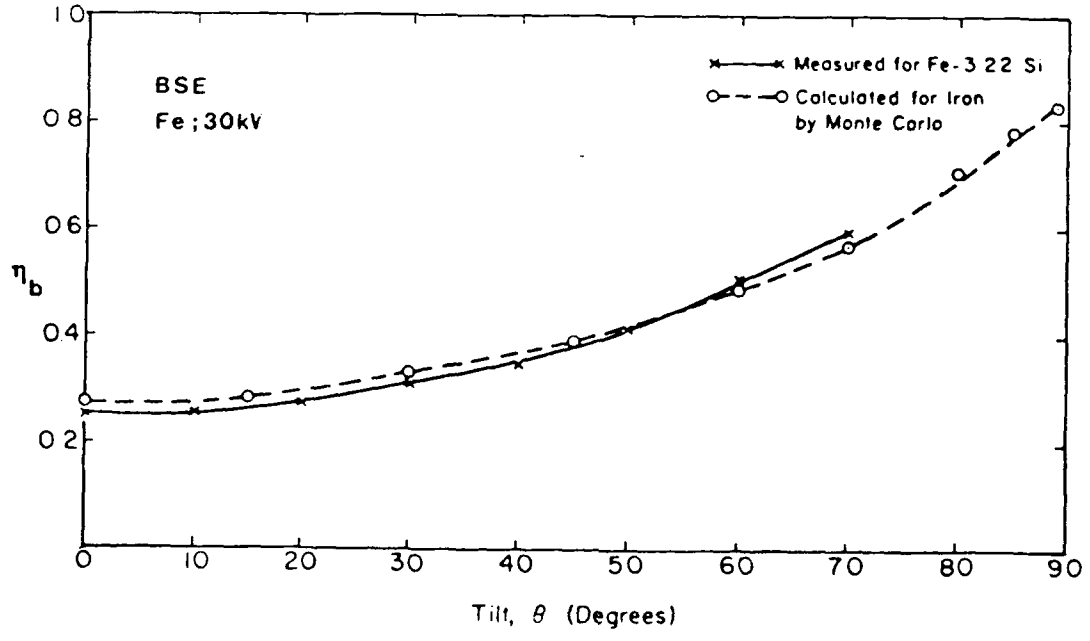

Fig.8 : Calculations of secondary electron and back-scattered electron yield for iron (Z = 26) as a function specimen tilt angle (away from normal incidence at θ = 0).

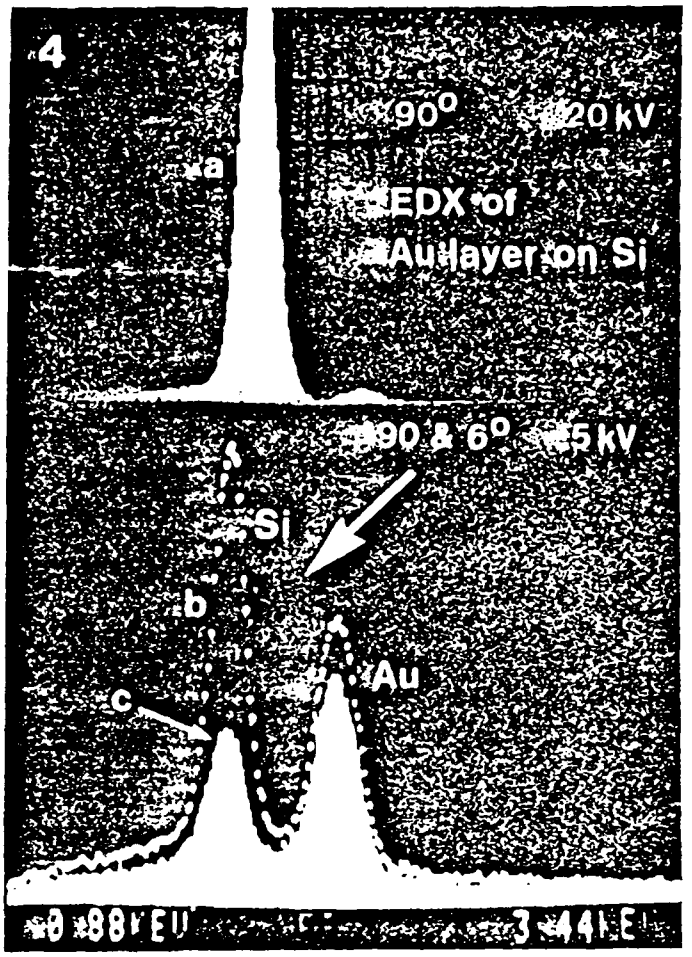

Excitation volume as a function of kV. X-rays (EDX) from a composite specimen with ~ 10nm Au layer on Si.

(a) 20kV normal (90°) incidence - very small Au signal

(b) 5kV at 90° - substantial signal from Au surface film

(c) 5kV at glancing incidence of 6° (semi-RHEED conditions with penetration equivalent to 500V at 90°) - Au signal is dominant peak in spectrum: beam energy still sufficient to excite Au(M) and Si(K).

The lack of Au/Si ratio sensitivity to tilt in the range 3-6° indicates mixed Si-Au surface with island formation or alloying between the elements.

Fig.9 : EDX x-ray microanalysis of ~10nm thin film of gold on a silicon substrate.

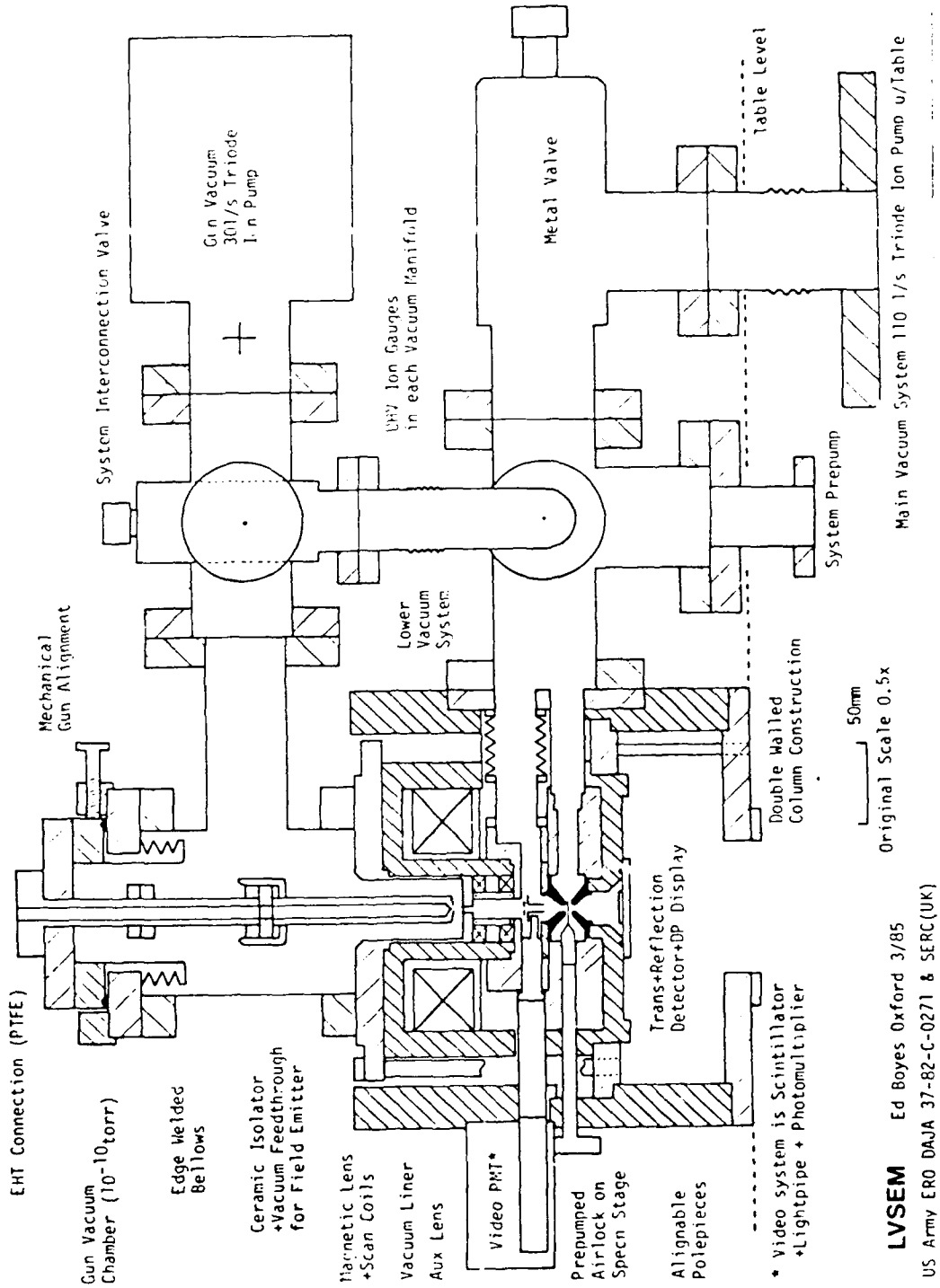

Fig.10 : General arrangement vertical cross-section diagram of main part of LVSEM column and vacuum lines.

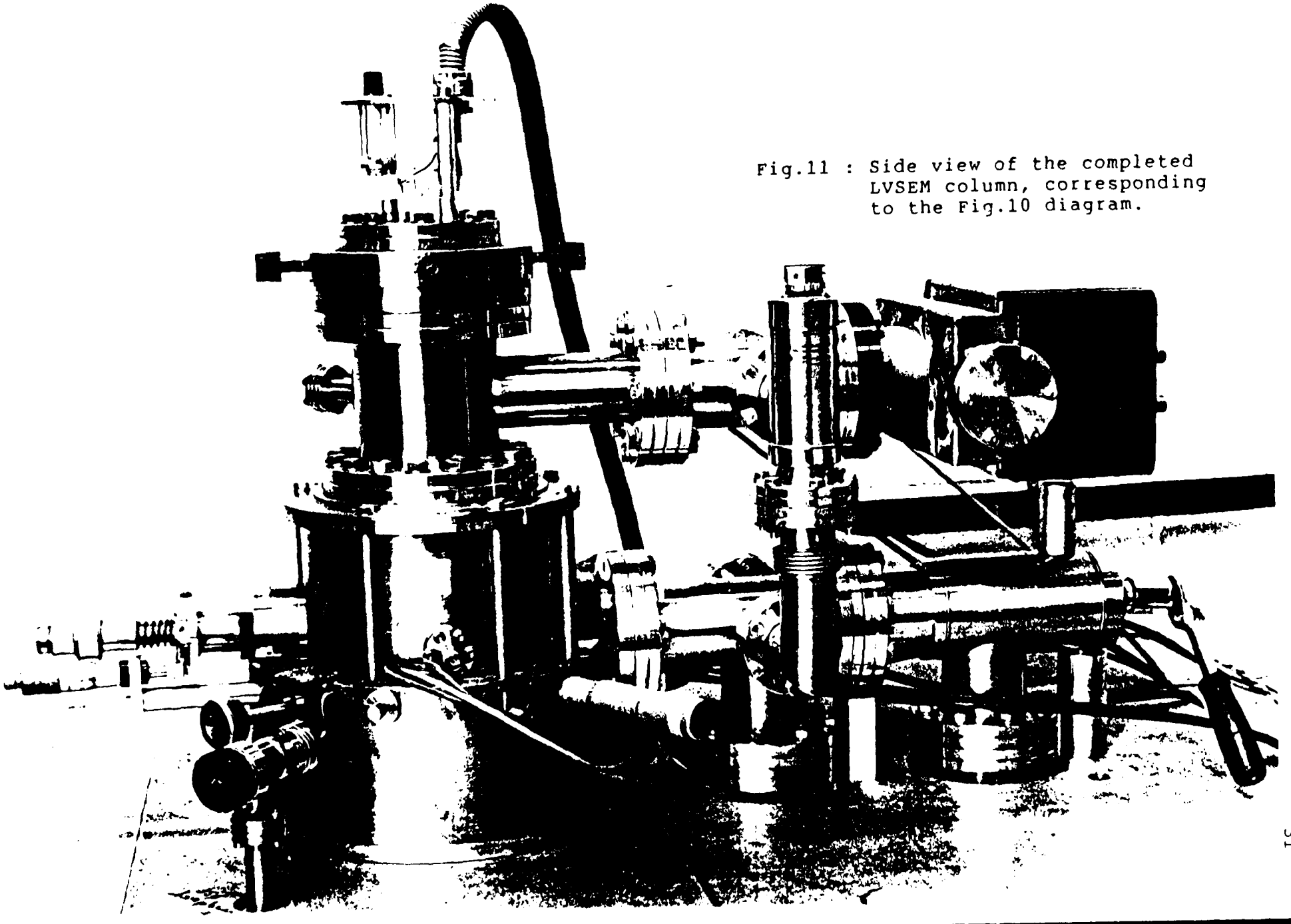

Fig.11 : Side view of the completed LVSEM column, corresponding to the Fig.10 diagram.

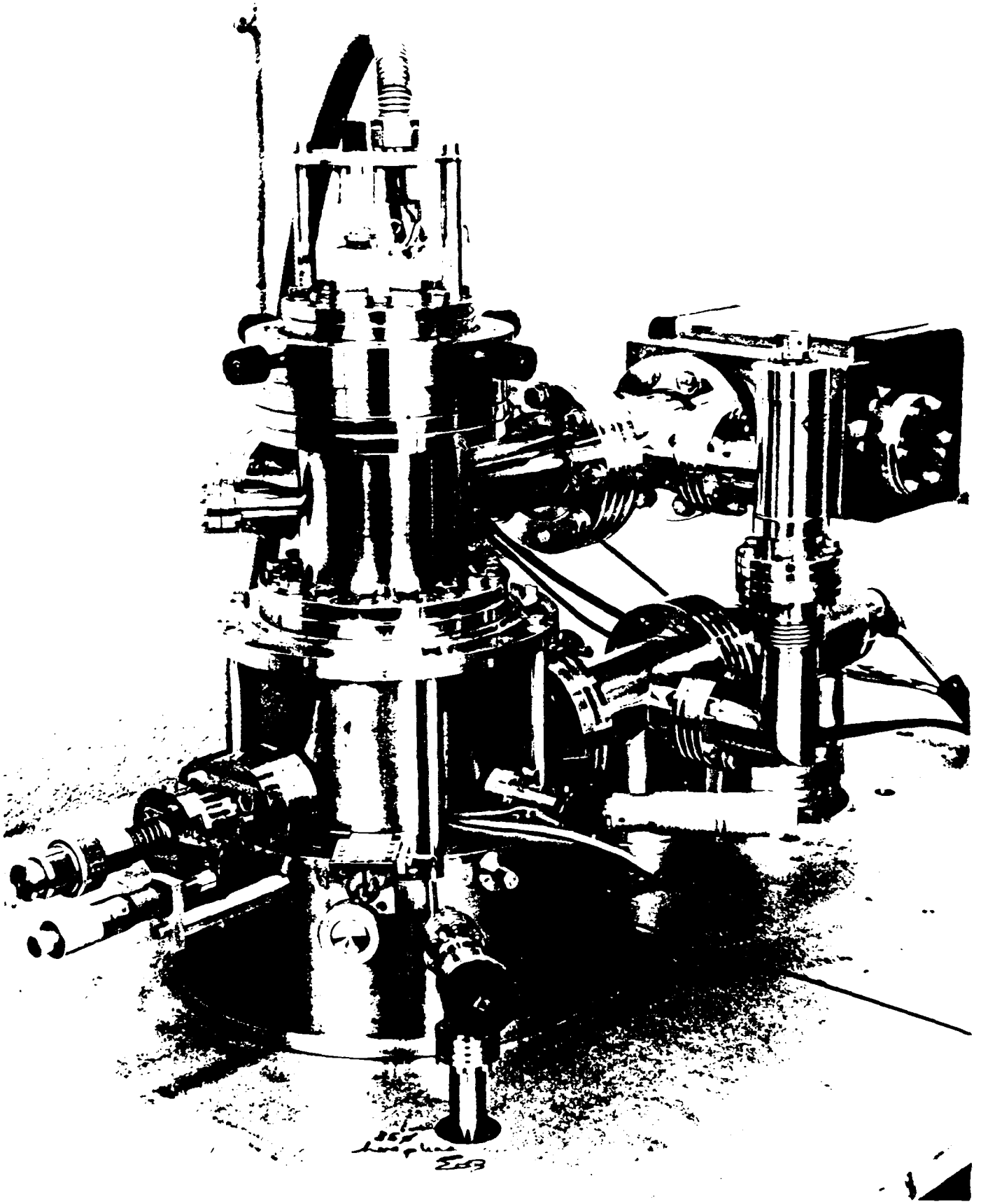

Fig.12 : Front of LVSEM column.

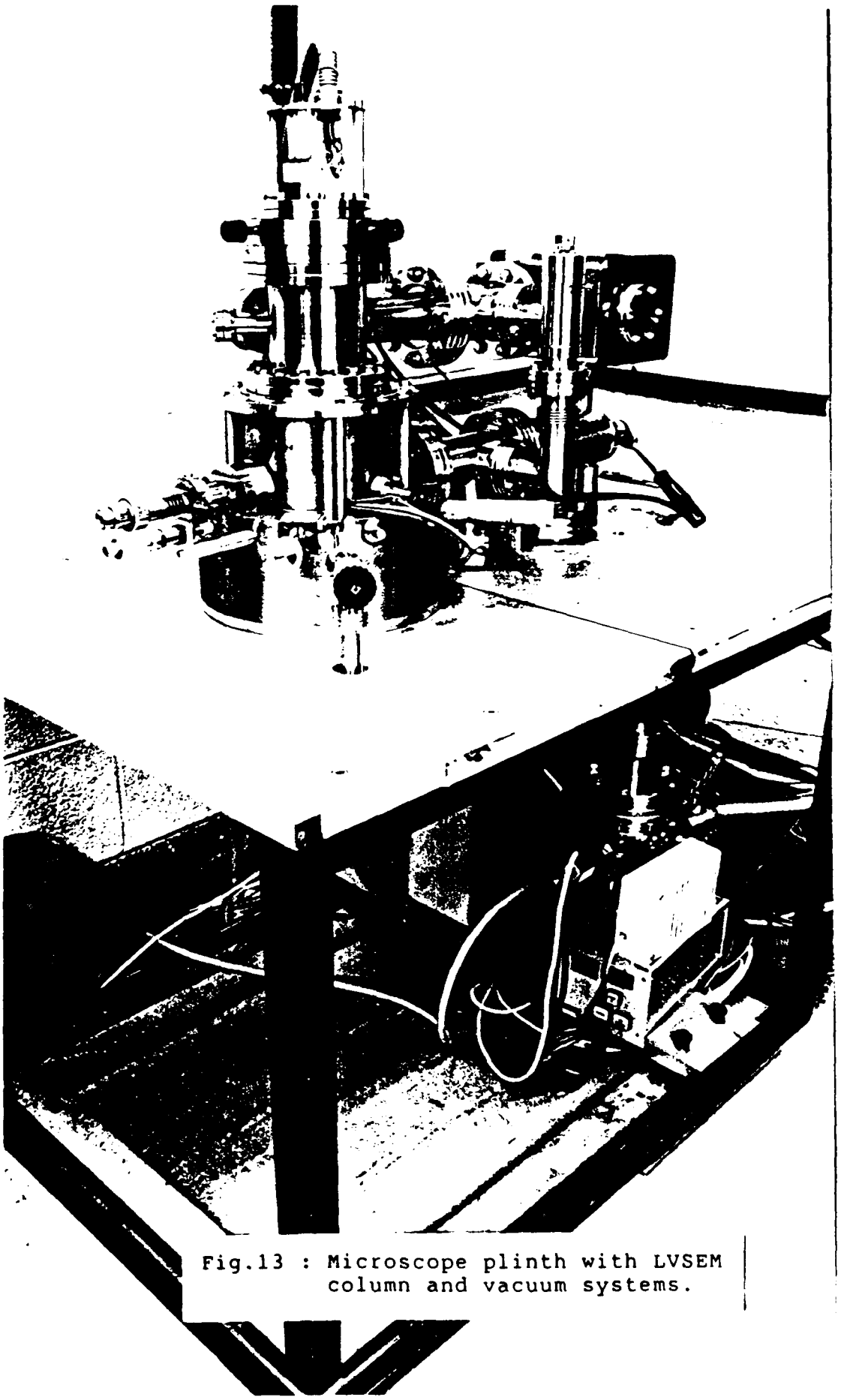

Fig.13 : Microscope plinth with LVSEM column and vacuum systems.

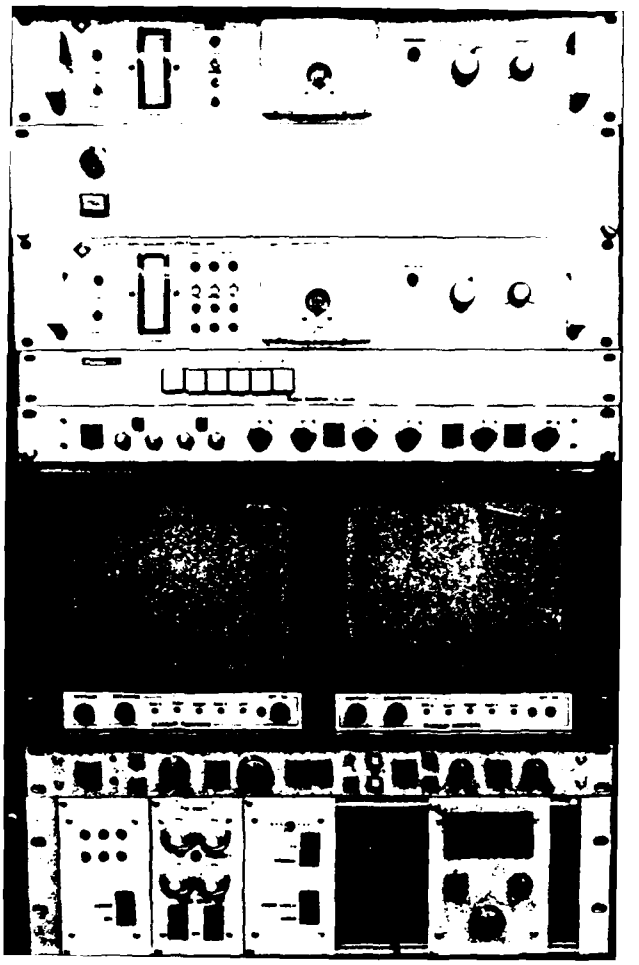

Fig. 15 : [Summary of LVSEM design specification - from poster at 11th ICEM, Kyoto, Japan, 1986].

ENGINEERING FOR LOW VOLTAGE SEM

* MINIMUM INNOVATION

* VOLTAGE ENGINEERING IS SIMPLIFIED

AC FIELDS

* Analogue & digital SCANNING is phase lock synchronised to local AC mains frequency.

* Short COLUMN geometry.

* Double wall SCREENING.

* High DEMAGN/short focal length in final LENS.

* SITE.

CONTAMINATION OF SPECIMEN & MICROSCOPE

* Clean, dry, ion-pumped VACUUM systems.

* Prepumped AIRLOCK specimen exchange.

* In-situ specimen PREPARATION may be necessary.

* Low voltage is more SENSITIVE to contamination, but what is the effect of voltage on PRODUCTION ?

  The real problem may be with specimens previously examined in conventional systems at high voltage.

LENS EXCITATION AT LOW VOLTAGE

* RELATIVE excitation can be very high ($NI/\sqrt{Vr} > 200$), without problems of high ABSOLUTE excitation.

* NI remains low (<4000At).

* Little SATURATION (Bm <1T).

* Conventional power supplies.

* Power dissipation/COOLING is OK.

* Super performance LENSES, eg Cs=0.15mm, in enhanced SECOND (& higher) ZONEs, but only at <5kV.

Fig.16 : Image of cement fracture sample imaged uncoated and without charging artefacts at 1kV. Scale is 0.1mm.

10. REPRINTS OF PUBLICATIONS

List of Papers Published and included in Appendix.

1. E D Boyes, On-line digital imaging; Nature 304 (1983) 289.

2. E D Boyes, High resolution low voltage scanning electron microscopy (LVSEM); Inst of Phys Conf Ser 68, Proc EMAG 83 (1984) 485.

3. P J F Harris and E D Boyes, Electron microscopy of a real platinum/alumina catalyst; ibid 275.

4. E D Boyes, M J Goringe, J J Gill, B J Muggridge, J P Northover and C J Salter, Slow scan applications of a digital video framestore system; ibid 211.

5. E D Boyes, High resolution at low voltage : the SEM philiosopher's stone; Proceedings of the 42nd Annual Meeting of the Electron Microscopy Society of America (Detroit, 1984) and published San Francisco Press (1984).

6. E D Boyes, P L Gai and C A Warwick, Cathodoluminesence of catalyst crystallites; Nature 313 (1985) 666.

7. E D Boyes, M D Hill, M J Goringe and C J Salter, Sub-micron backscattered electron microanalysis in the SEM; Inst of Phys Conf Ser 78, Proc EMAG 85 (1985) 243.

8. E D Boyes, The potential of the low voltage scanning electron microscopy (LVSEM), MICRO-86; abstract publd Proc Royal Microscopical Society (1986).

9. E D Boyes, The potential of low voltage scanning electron microscopy (LVSEM); Proc XIth International Congress on Electron Microscopy, Kyoto, 1 (1986) 383

10. P L Gai, S E Male, C J Salter, N J Long and E D Boyes, Microstructures of high Tc Y-Ba-Cu-O superconductors, Inst of Phys Conf Ser 90, Proc EMAG 87 (1987) 307.

Additional (4) publications are being prepared as staed in the Summary to this report.

NATURE VOL 304 21 JULY 1983

On-line digital imaging

Ed Boyes looks at digital image processing — the technique which gleans quantitative data from pictures.

DIGITAL techniques are increasingly being used to enhance, standardize and sometimes replace conventional photographic recordings. This growing interest in digital analysis arises largely from the fact that image processing puts a quantitative value on an otherwise qualitative picture, making it possible to compare two photographs accurately, or to glean more detailed information from a single image.

The essential difference between conventional photographs and digitally-processed images is that in the latter the image is converted to a digital form and stored as numbers in a large semiconducter image memory, or "framestore" attached to a computer, rather than being exposed directly onto a piece of film or an instant film pack. With typical commercially available equipment this means that images of at least 512 × 512 picture points, or pixels, can be quantified and stored directly from virtually any input, such as a TV camera or an ultra-sound scanner. The picture can be analysed with 8-bit precision, by splitting the image into 2^8 (or 256) shades of grey or colour before it is stored, with a chance of "doctoring" the image both immediately after input and again before output. In this way the image can be changed before an actual picture is produced, so that areas of interest can be enhanced and the background subdued, or colours can be added to increase contrast. Image processing also provides the opportunity to present other physical values in a visual form.

Advantages

Image enhancement procedures are designed to produce the best possible image from the input, and to assist the analysis and communication of results. In doing so, digital techniques have three major advantages over conventional techniques. First, once the data have been in the computer, the images are available for processing in any order with random access to the memory, unlike conventional films which have to be analysed in sequence. Second, image sequences can be displayed on the video screen and frozen electronically at any time for closer inspection. Third, the original data is kept intact and can be repeatedly analysed without distortion. Furthermore, any analytical procedures used on the data can be explicitly defined and recorded.

Enhancement techniques

At the most simple, but nevertheless essential, level of data processing, the brightness and contrast of the image are enhanced so that features of special interest can be picked out more easily. More complicated imaging needs more advanced techniques. Many scientific signals are either very infrequent or very weak, coming complete with heavy background noise. To break these down requires long integration times, during which the image is built up in the memory store and controlled from the display on a video screen. Signal to noise ratios can be improved by averaging successive frames from a TV camera with a controlled output or by summing the data from adjacent pixels, which brings out the similarities in the data and hence the differences between the data and the background. When the noise level of the input is lower, a modified processing of adjacent pixels, for example in a 3 × 3 array, can be used to sharpen edge-detail by enhancing the differences rather than the similarities between the groups. Similarly, information about intensity may be made more meaningful by producing a non-linear output. An example of this would be in an experiment where the temperature was being increased from 0 to 1,000°C, but in which it was important to see the point at which 600°C was reached. This changeover would be made more obvious by representing, for example, all temperatures below 599°C by the colour green and all those above 600°C by the colour red.

Clearly, digital image processing is a useful analytical technique. It therefore seems curious that it has only become widely used in the last few years, even more so when you consider that analog electronic analysis has been in use far longer, despite the fact that it can only analyse serially and the information that it gives is much less useful. The problem with developing digital techniques has been that until recently, digital image processing has required a substantial mainframe computer, and, even then, there were only facilities for on-line analysis and control in very specialized applications. Now, however, laboratory-scale systems are available with typical image memories of 512 × 512 or 1,024 × 1,024 pixels. Each picture point from the input is mapped to an equivalent position on the computer video screen. If the input frequency is slow, the image processing can be carried out by computer alone. This gives a highly flexible system, but severely limits the rate at which data can be handled. To reach the 15 MHz required by a raster scan demands that some flexibility be sacrificed by the introduction of a piece of dedicated hardware, such as the recursive video processor, or RVP.

The RVP is essentially capable of doing three things — it can take the difference between adjacent frames, and it can sum or average incoming signals to improve the signal to noise ratio. Averaging the signal involves taking data from the store and comparing it with the incoming data, so that, for example, one eighth of the output comes from the input data and seven eighths from the running average. In addition to controlling noise, it is important to avoid distortion of the image during processing. Any digital processing system is capable of generating a picture without an input, and so it is essential to make sure that interference is kept to a minimum.

It seems that in the future, digital imaging techniques will split into three main categories with cost being their main divider. First, there will be the simple units to store or compare single images in digital form with a TV output display. These are now becoming available as single computer cards, similar to those upon which the latest high-resolution colour VDUs are based. Second, when any significant level of processing becomes necessary, some kind of computer will have to be involved, and this in turn will require extensive software, suggesting that some kind of package system will be developed. At the third level will come the highly sophisticated, fully integrated sytems with powerful processors attached to multiple framestores and extensive processing, analysis and storage facilities.

Luckily, it is emerging that many image processing methods require very similar hardware and software. It appears that all that is needed to specialize the systems is a tailor-made sensor coupled to personalized software.

Ed Boyes is from the Department of Metallurgy and Science of Materials of the University of Oxford, UK.

Inst. Phys. Conf. Ser. No. 68: Chapter 12 485
Paper presented at EMAG, Guildford, 30 August - 2 September 1983

High resolution low voltage scanning electron microscopy (LVSEM)

E D Boyes

Department of Metallurgy & Science of Materials, University of Oxford, Parks Road, Oxford OX1 3PH, England

The choice of accelerating voltage for secondary electron imaging of surfaces in a conventional SEM is often something of a compromise, particularly for samples which are essentially non-conducting e.g. structural ceramics and related materials such as cement, Fig.1, or biological material. The ability of an instrument to form the small sized probe needed for high resolution imaging[1-3] depends on the exact configuration, but generally is significantly improved at higher voltages, with a typical minimum of a few nanometres at 20-100kV. However, at these accelerating voltages the secondary electron yield of most materials is very low, typically < 0.1, leading to severe surface charging problems with non-conducting regions of specimens, the images of which are consequently of poor quality. Conversely at very low voltages of 0.1-3kV secondary electron yields are high and generally close to unity, minimising surface charging but the optical performance of the conventional SEM is often rather poor, typically < 0.1 micrometer. In many practical applications high voltages are used and specimens are coated with a conductive metal film to control charging, but this can modify high resolution surface detail, not always to advantage; suppresses some potentially useful contrast modes and complicates microanalysis. A new type of high resolution scanning electron microscope designed to operate primarily at low voltages - an LVSEM - is therefore required. This paper considers some of the possibilities.

The theoretical performance of an electron-probe system with an optimised source can be described by an equation of the type:

$$d = \sqrt{\left\{\frac{4i}{\beta V \pi^2 \alpha^2} + \left(\tfrac{1}{4} C_s \alpha^3\right)^2 + \left(C_c \frac{\Delta V}{V} \alpha\right)^2 + \left\{\frac{0.61\lambda}{\alpha}\right)^2\right\}} \qquad (1)$$

where C_s and C_c are respectively the spherical and chromatic aberration coefficients, α is the probe semi-angle (sr), β is the effective source brightness ($A/cm^2/sr/volt$), V and ΔV are the accelerating voltage and energy spread of the beam and λ is the electron wavelength corresponding to V. For these calculations a probe current (i) of 1×10^{-11} Amps (10pA) was used; smaller currents may be practical at low voltages and by using a digital imaging system. The 10-90% risetime at an edge[4] can be better than the point resolution (d) by a factor of ~ 3, depending on the current and its distribution and these values are also of interest as the accepted SEM resolution test. Equation (1) can be re-written as:

$$d = \sqrt{\{B + S^2 + C^2 + D^2\}} \qquad (2)$$

Each term has a dependence on both accelerating voltage (V) and aperture semi-angle (α), but in practice it is desirable to select V independently to optimise the interaction with the specimen and to maximise the current by choosing the largest aperture consistent with acceptable geometrical aberrations for a given magnification (Figs.3 and 5). The electron-optical aperture is still very small compared to the optical microscope, preserving a substantial depth of field.

Interaction with the specimen in terms of the excitation volume, of which Fig.4 is an example; sensitivity of surface imaging and secondary electron production efficiency[5] are optimised at low voltages, often below 3kV and sometimes $<<$ 1kV. Image-distorting surface charging is then largely avoided since between the E_1/E_2 cross-over potentials[5] the total electron yield is stabilised at unity by a small positive potential related to the work function. This negative feed-back is typically less than one volt and small enough to be insignificant. The precise energies, including E_1/E_2, depend sensitively on the material and treatment of each specimen[5-7]. At very low voltages of ~ 1kV, radiation damage to MOS semiconductor circuitry is effectively eliminated, allowing 100% functional inspection of microchips[8]. Backscattered imaging should also be improved.

Low voltages produce images which are significantly more surface localised; reduce the effective spread of the beam interaction, largely eliminate the secondary background due to backscattered electrons[16] and restrict beam breakthrough at surface steps or thin layers, enhancing image contrast. As a consequence the image resolution at low voltages should be very similar to the probe-size, which is not always the case at high voltages[3]. For a given probe current the higher secondary yields at low voltage improve the signal to noise ratio (S/N) by an order of magnitude or more, largely compensating for the lower specific brightness (β.V). Unfortunately under these conditions the probe size of a typical SEM may be unacceptably large, at 0.1 micrometer or more, primarily due to chromatic aberration, Fig.3(b), and there may well be other operational limitations[9] associated with the aperture dependent probe current, susceptibility to external AC magnetic fields, contamination of microscope and specimen etc.

Conductive coating techniques - the traditional solution to this dilemma - are somewhat variable in effect[10]. They preclude looking at supported metal particle catalysts, a major potential application, or obtaining chemical information[7]; complicate any subsequent microanalysis e.g. of battery aluminas or cement-based materials; must be avoided if semiconductor devices are to be operated e.g. after a quality control evaluation, and at the highest resolution they may introduce a characteristic surface texture of their own[10]. However, controlled shadowing can be used constructively to enhance low contrast detail. It is a bit like interpreting the image of a countryside scene after a snow storm: some features are revealed, some modified and others lost altogether. High voltage beam breakthrough or image blooming at the edge of features can lead to serious errors in metrology[11].

A re-examination of the electron-optical principles[9 12-14] involved, Figs.3(c,d) and 5, has shown that it is feasible to design a new type instrument - the LVSEM - which avoids most of these problems by providing a projected low voltage resolution in the nanometre range, fully comparable to that achieved with conventional SEMs at high voltage, whilst using only readily available established technology with a minimum of component

Fig.1. Defect in cement, uncoated 1kV low magn. (scale is 0.1mm)

Fig.2. High resolution of low contrast Al-[illegible] TEM/SEM 100kV (0.2[illegible]

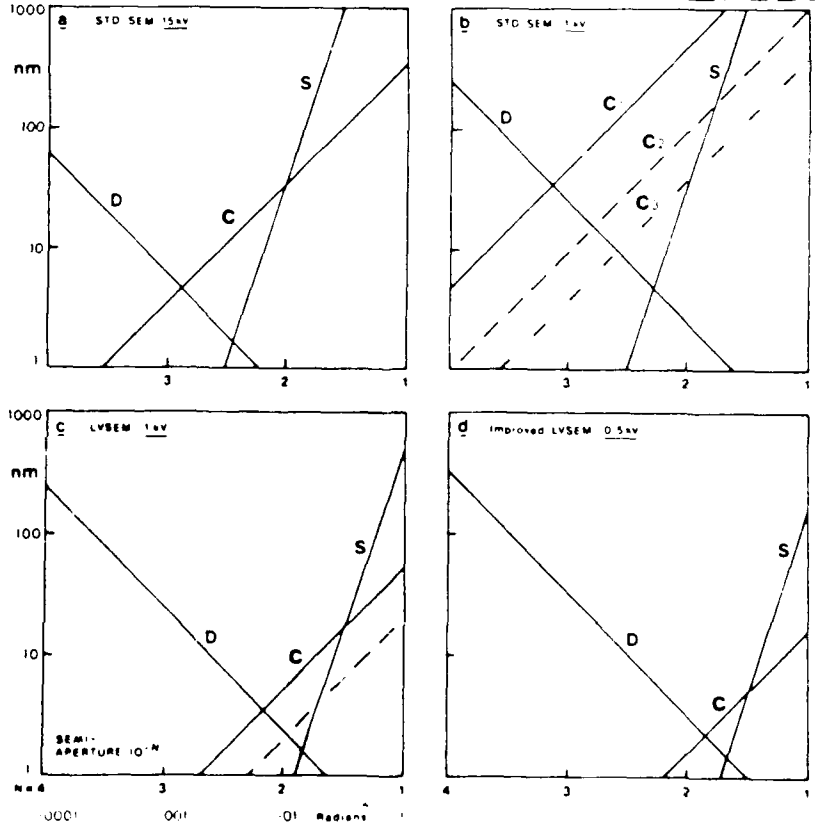

(a) 15kV C_S=75mm C_C=20mm ΔV=2.5eV Std SEM.
(b) 1kV Std SEM ΔV=2.5(0.5,0.2)eV.
(c) 1kV C_S=C_C=1mm ΔV=0.5(0.2)eV LVSEM.
(d) 0.5kV C_S=0.27mm C_C=0.4mm ΔV=0.2eV.

Fig.3. Relative importance of contributions to SEM probe size

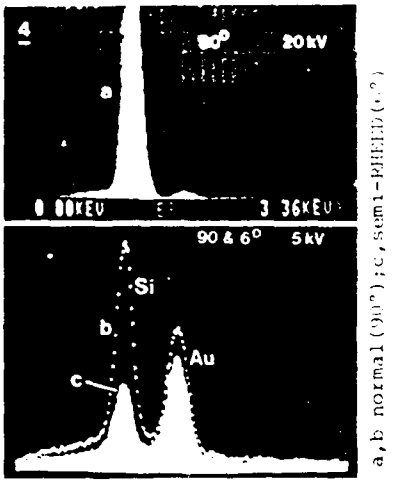

Fig.4. Excitation volume, X-rays 20/5kV, ~ 10nm Au on Si.

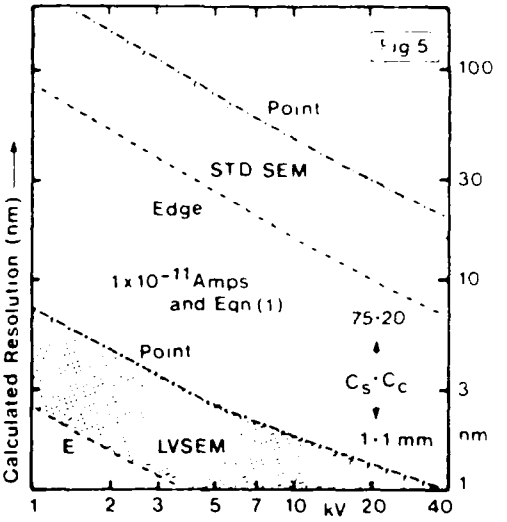

innovation. It has been found that at low voltages (V < 10kV) very high relative excitations of $NI/eV_R \sim 30$ can easily be used to produce extremely low aberration coefficients in conventional (non-superconducting) second-zone condenser-objective lenses (e.g. C_s = 0.27mm, C_c = 0.4mm (Fig.3(d)) with specimens up to a few millimetres in thickness and highly efficient secondary electron collection[15]. The practically important aperture condition is also relaxed. The system under construction is based on a field emission gun of suitably high brightness and low energy spread; a low aberration optical design with C_c held below 1mm and other appropriate engineering, including AC field protection and dry bakeable vacuum systems.

Acknowledgements

This project has been made possible by support from the SERC(UK) and by a grant from the European Research Office of the US Army. Discussions with Professor Sir Peter Hirsch FRS; calculation assistance from Mr S Thoms and a chance encounter with ref.9 by A P Wilska are gratefully acknowledged.

References

1. R F W Pease and W C Nixon, J.Sci.Instr. 42 (1965) 81.
2. A N Broers, J.Vac.Sci.Technol. 10 (1973) 979.
3. C J Catto and K C A Smith, J.Microsc. 98 (1973) 417.
4. J Bentley and R W Carpenter, Proc.37th Ann EMSA (1979) 566.
5. R Kollath, Z.Physik 38 (1937) 202.
6. P H Dawson, J.Appl.Phys. 37 (1966) 3644.
7. Y Ishikawa, N Awaya, Y Nakazawa, H Yamadera and T Ichinokawa, Surface Science 124 (1983) 87.
8. K Ura Hitachi, Instrument News 5 (1980) 2.
9. A P Wilska, J.Microsc. 83 (1964) 207.
10. B J Panessa-Warren and A N Broers, Ultramicrosc. 4 (1979) 317.
11. V Coates, Proc.40th Ann.EMSA (1982) 752.
12. A V Crewe, Ultramicrosc. 1 (1976) 267.
13. J E Barth and J B Le Poole, Ultramicroscopy.
14. N Tamura et al, Electron Microsc. 1980 1 520.
15. H Koike, K Ueno and M Suzuki, Proc.29th Ann.EMSA (1971) 28.
16. L M Welter and V J Coates, SEM/1974 59.

Inst. Phys. Conf. Ser. No. 68: Chapter 8 275
Paper presented at EMAG, Guildford, 30 August - 2 September 1983

Electron microscopy of a real platinum/alumina catalyst

P J F Harris and E D Boyes

Department of Metallurgy & Science of Materials, University of Oxford, Parks Road, Oxford OX1 3PH England

1. Introduction

The potential of transmission electron microscopy for studies of supported metal catalysts has long been recognised (Adams et al, 1962), but progress in the field has been slow. This is probably due in large part to the difficulties associated with preparing suitable specimens from these hard, porous materials. Traditionally, simply grinding the catalyst and depositing it onto a carbon film has been used. However, the action of grinding may disrupt the catalyst morphology (for example, the pore structure of the support may be destroyed) and a uniform coating of catalyst over the carbon film is often difficult to obtain. Moreover, contrast from the carbon film itself may be a disadvantage in high resolution studies. While there have been many studies of model catalysts, where the metal particles are vapour-deposited onto an idealised support film, the relevance of these studies to a real catalyst with a microporous support has not yet been fully established. In this paper we show how a new technique may be used to prepare thin films of a real platinum/alumina vehicle exhaust catalyst, and outline the ways in which this technique has facilitated studies of the growth and structure of the platinum particles. The procedure is based on a process for applying catalytic coatings onto metallic substrates for use in exhaust emission control units (Nelson et al, 1981).

2. Specimen Preparation

The two starting materials were an aqueous alumina sol (270g/litre) and crystals of tetrammine platinous chloride. The platinum complex was dissolved in a small amount of water and then thoroughly mixed with the sol. Stainless steel microscope grids were then dipped into the mixture and withdrawn with a thin liquid film suspended across the grid squares. This was then dried, fired in air at 600°C and reduced in flowing hydrogen at 500°C. In this way very thin self-supporting sheets of catalyst could be formed across parts of the grid. Fig.1 shows a low magnification micrograph of a typical specimen, which contains a number of the sheet-like regions. As can be seen, these regions were often tens of microns in extent, and the thickness was generally less than 30nm. Therefore, further thinning of the specimens, which might modify the structure, was not necessary. Stability of the specimens under a focused electron beam was usually found to be good. Fig.2 shows a high magnification micrograph of a typical thin specimen; here the strongly diffracting supported particles can clearly be seen against the thin, weakly diffracting support. The porosity of the support shows up well in this micrograph and there is no carbon film to detract from image clarity. Fig.3 shows the particle size distribution for fresh specimens, there was very little variation in

the distribution from specimen to specimen. Hydrogen surface area measurements have been carried out on the bulk material, and are found to be in close agreement with particle size measurements from TEM (Harris et al, 1983).

3. Platinum Particle Sintering

Sintering of the supported particles is a serious cause of catalyst deactivation, and much effort has been devoted to identifying the mechanisms of growth. Specimens prepared by the new technique have proved to be well-suited to sintering studies since micrographs of the sheet-like regions enable the diameters of a large number of platinum particles to be rapidly measured. The shapes of the resulting particle size distributions, and the variation of the mean diameter with time, can lead to valuable insights into the mechanism of sintering. A previous study of sintering behaviour in air at 600°C (Harris et al, 1983) led to the conclusion that a change in the mechanism from migration and coalescence of whole particles to interparticle transport of individual platinum atoms or platinum oxide molecules probably occurred after about 2 hours, when the mean particle diameter was 7.4nm. An interesting feature of that study was the discovery of abnormally fast-growing particles, which could reach sizes in excess of 50nm after 24 hours. The particles were usually plate-like in shape, and microdiffraction analysis suggested that they possessed a twinned structure. More recent work has shown that the growth of large plate-like particles becomes even more important at temperatures higher than 600°C. In Fig.4 we show a specimen heated in air at 700°C for 8hours, where particles as large as 100nm can be seen. Similar fast-growing particles have been observed in previous studies of model platinum/alumina catalysts (e.g. Wynblatt, 1976). The growth mechanism for these particles almost certainly involves interparticle transport rather than migration and coalescence, and it seems likely that in some cases the accelerated rate of growth results from the presence of twins. Abnormal growth could be a major problem in an operational vehicle exhaust catalyst since temperatures in excess of 600°C are often encountered. Scanning electron microscope studies have confirmed that large particles grow on the surface of the bulk material; Figs.5(a) and (b) show typical high resolution SEM micrographs.

4. Platinum Particle Structure

The structures of the supported particles may be important in determining both the reactivity and sintering behaviour of the catalyst. They may also help to characterise mechanisms of nucleation and growth. The thin specimens prepared by the new technique often enabled particle structures to be identified from bright field micrographs. The most commonly recognised structure in both fresh and sintered catalysts was the truncated octahedron, an example of which is shown in Fig.6. A wide variety of twinned particle structures were also observed, including decahedral particles of the type frequently seen in model catalysts (Marks and Smith, 1983). Fig.7 shows such a particle, from a specimen sintered for 24 hours at 600°C. More detailed structural information may be obtained from TV assisted lattice imaging, and the specimens have been found to be well suited for this purpose (Harris and Boyes, to be published). A lattice image of a singly-twinned particle is shown in Fig.8.

5. Conclusions

The new technique has advantages of relative simplicity. The direct preparation of TEM specimens avoids the necessity of any further thinning which might modify catalyst morphology. It has been possible to apply to

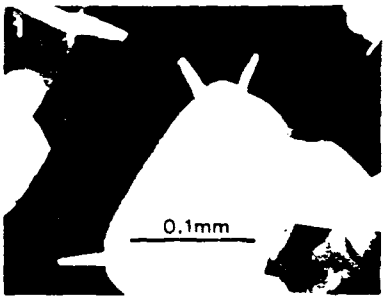

Fig.1,2 Low and high magnifications of typical fresh specimen.

Fig.3 Fresh PSD.

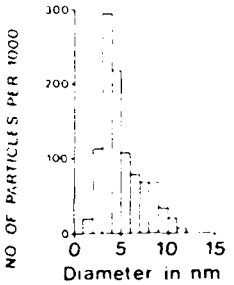

this real catalyst most of the characterisation techniques which have previously only been widely used with model systems. Some of them are more difficult to use, primarily due to the nature of the support and the absence of a consistent particle orientation. However, the results are obtained from real material and can be compared directly with the chemical data from larger samples. Since the specimen is composed entirely of catalyst material, sequences of heat treatments can be followed, including in situ in the HVEM environmental cell. Some of the features such as abnormal growth and decahedral multiply twinned particles are similar to those previously seen in model systems, although the proportion of such particles may be modified. This confirms the value of the earlier structural work on model systems and comparison of results using different forms of substrate may help to elucidate growth mechanisms.

Acknowledgements

Dr J A Cairns of the Chemistry Division, AERE Harwell, is thanked for provision of materials for specimen preparation and many stimulating discussions, and the SERC and AERE Harwell for supporting the work.

References

Adams C R, Benesi H A, Curtis R M and Meisenheimer R G 1962 J.Catal. 1 336
Harris P J F, Boyes E D and Cairns J A 1983 J.Catal. 82 127
Harris P J F and Boyes E D to be published
Marks L D and Smith D J 1983 J.Micros. 130 249
Nelson R L, Ramsay J D F, Woodhead J, Cairns J A and Crossley J A A 1981 Thin Solid Films 81 329
Wynblatt P 1976 Acta Met. 24 1175

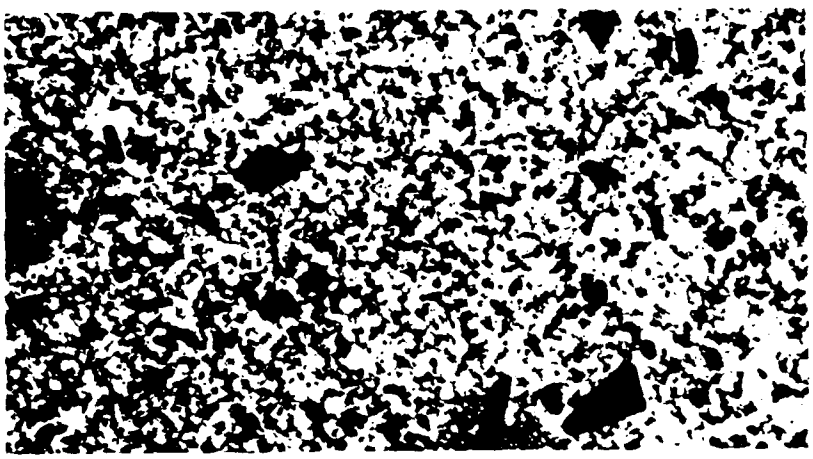

Fig.4 Sintered in air for 8 hours at 700°C.

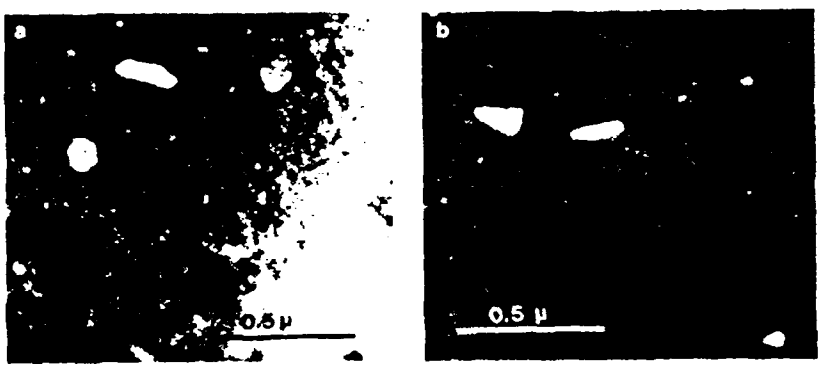

Fig.5 SEM of abnormally large surface particles.

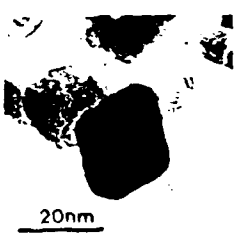

Fig.6 Octahedra.

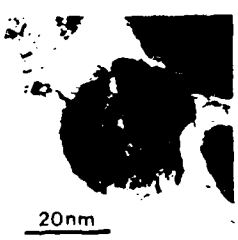

Fig.7 MTP.

Fig.8 Single twin (lattice image).

Inst. Phys. Conf. Ser. No. 68: Chapter 7 211
Paper presented at EMAG, Guildford, 30 August - 2 September 1983

Slow scan imaging applications of a digital video framestore system

E D Boyes, M J Goringe, J J Gill, B J Muggridge, J P Northover and C J Salter

Department of Metallurgy & Science of Materials, University of Oxford, Parks Road, Oxford OX1 3PH, England.

Conversion and computer readable storage of slow scan signals with a continuously updated image display or video recording at TV rate[1], is one of the functions available using a digital video framestore image memory in conjunction with a scanning electron microscope (SEM, STEM, AEM etc.) or other types of beam analysis equipment with raster imaging facilities, such as EPMA, AES, SIMS etc.

Each of the multiple framestore units has 512x512x8-bit memory locations and in the Micro Consultants Intellect-200 system[2-3] they can be stacked (to 16-bits) for greater depth, or for width or height (to 2048, e.g. 1024x1024); with any 512x512 section selected for display by smoothly scrolling it into the TV output processor window. The complete contents can be displayed by serially slow scanning through computer ports. Acceptable inputs are standard TV format (interlaced composite video); synchronised digital sampling of a wide range of analogue slow scans[1] with frame times < 0.2 seconds (Intellect 100) to > 0.5 hours; directly coupled digital scans (common pixel clock) with an unrestricted upper time limit or more slowly but with greater flexibility, e.g. reformatting, through the computer. At low magnification/resolution this can also be used to generate the primary slow scans via DAC cards with internal synchronisation via software, simplifying the use of a cursor to locate points, for example for microanalysis. With this system a separate signal multiplexer is required to use the single input processor for concurrent acquisition from multiple synchronised sources, e.g. from more than one detector, or this can be achieved independently through the computer. The ADCs of the input digitiser/processor can also be bypassed for direct counting.

Where stability is adequate, as it generally is in EPMA, co-ordinates on the specimen and in the image memory are equivalent. Previously only a live electron video image could be used to position the probe; but with a continuous real-time display independent of acquisition rate, chemically discriminating but weak X-ray maps; EBIC signals for electrical activity or bandwidth limited absorbed current total electron images, collected over 40 seconds or more, may be more sensitive. Fig.6 is an example of the use of an X-ray reference image, with a computer generated cursor marking the points from which quantitative X-ray microanalysis was obtained (full cursor at currently active position). At high magnification/resolution, e.g. STEM requiring a microscope related phase-locked pixel clock or faster scan rates, a separate digital scan generator which can be placed under computer control is used.

The continuous display of the on-line digital system combined with the flexibility of computer controlled and exactly defined processing is important in optimising image/data collection procedures, especially where there are detection bandwidth limits and exposure times are extended; or the signal is weak, Fig.3(b), or very noisy, Fig.4, so that repeated scanning is necessary to build-up a significant result. Figure 3(b) X-ray image is an integration of 32 frames (WDX) and was continuously monitored to achieve adequate S/N. Techniques previously considered to be almost impossibly difficult even to achieve focus, due to very long frametimes e.g. 50-500 seconds for EBIC at low voltages (6kV (Fig.7)) are now made practical using the framestore as a simple scan converter. Subsequent photographic recording, assisted by an electronic greyscale signal generator (Fig.2) is simplified and readily standardised[4].

Routines for noise reduction by spatially resolved time averaging during acquisition[1], are under software control, with direct operator involvement in selecting the appropriate conditions via a soft-key redesignation of the VDU numeric pad functions (Fig.1) and within the possibilities of the hardware, making TV rate, (Fig.4), more useable e.g. to reduce specimen charging and as an essential prerequisite to more sophisticated image processing. At any time the image can be frozen and stored digitally for subsequent processing or analysis, including geometrical, which can be fully quantitative to the level of the pixel spacing, luminance discrimination and statistics, since no corruption is involved in the recording process. In effect a data base is created. Excellent linearity (Fig.2) is achieved in the input digitiser. Fig.3(a) overlay illustrates post-acquisition line scanning, with one degree of smoothing applied to improve the significance. Pixels can also be averaged multi-dimensionally.

The typical 'spotty' low density selective X-ray image can be displayed unmodified with a large number of pixels for the best spatial resolution or processed by combining the data from adjacent pixels to enhance the signal-to-noise ratio·(S/N) and improve the chemical precision or discrimination of phases, within the limitations of any corrections. Providing the original data has been acquired at high enough resolution, these decisions can be taken with the powerful assistance of computer-aided on-line analysis (and direct visual observation!), without in anyway corrupting the digitally stored information. The results can be used to control data acquisition interactively or automatically e.g. statistical precision. Unlike in a photograph, inadequate data in the store is not lost but can be added to by repeated scans; which is particularly useful for beam sensitive materials. No potentially useful data need be lost (16-bit dynamic range is 65536) and repeated analysis or trial display processing of the securely stored data is possible. This is a consequence of the separation of the sensor, recording and display functions which are non-linear and inflexibly integrated in direct photography.

More precisely defined and exactly reproducible image processing procedures (intensity scale adjustments, making full use of the multiple bit planes, e.g. compression, offset black level, expansion/luminance zooming, derivative, ratio, difference, slicing, smoothing, enhancement and non-linear or discontinuous amplification, γ, etc.) are possible in the digital domain, whilst software control through the PDP 11/23 computer and random access to the multiple framestores provides much greater flexibility. For example image enhancements e.g. matrix operations such as 3x3 sharpening of features using a local neighbourhood difference operator;

pixel noise smoothing or averaging, contouring, derivatives and reconstruction etc. can now be non-directional in output, assuming similar x and y input frequencies. Separate units may no longer be required for each signal processing function. Pixel replication and interpolation provide selective magnification.

Standard geometrical analysis procedures such as particle counting, areas (Fig.5(b)), histograms (Fig.5(a)) etc. are also available with these systems by slicing the processed luminance scale appropriately (Fig.5). Similarly there is a full range of fast graphics and image annotation features, which have been used in the preparation of some of the illustrations. As an aid to interactive control, overlays, cursors etc. (e.g. Fig.6) can be generated and moved at TV line rate on the output, rather than at the much slower input frame update rate. Fig.5 combines image processing and luminance slicing calibrated by X-ray microanalysis to define and identify chemically distinct areas for quantitative image analysis. This is an example of the use of microanalysis to calibrate the image luminance in terms of chemical composition. Clearly the use of a highly stable beam at normal incidence on the clean and carefully polished flat surfaces with minimal topography typically required for the most accurate quantitative X-ray microanalysis in the EPMA, optimises Z-contrast. The advantages of using calibrated predominantly backscattered electron images of this type are improved spatial resolution due to a reduced effective excitation volume; much higher cross-sections, up 10^2-10^5X compared to X-rays and better geometrical detection efficiency (10^2-10^3X) of signals. They are particularly useful for discriminating between distinct phases characterised by substantial differences in the major elements, since they depend on the sensitivity to mean atomic number (Z). Fig.5 is an example of well separated phases. The technique is not useful for minor elements, although secondary electrons sometimes maybe[5].

Routines are developed in software and implemented using the full system. As with the TV acquisition mode, the computer controlled system has various processing levels, each with a characteristic rate. At the full input speed, including TV, are hardware functions set-up with software controlled parameters (e.g. RVP, output processor LUT); routing through the computer accesses other devices e.g. dedicated FFT module and digital magnetic storage media, whilst the greatest flexibility but lowest speed is provided by using the computer directly for processing, but this is still quite practical for many slow scan applications. Colour can be added to highlight the analysis and communication of results.

It is probable that digital imaging will become standard for slow scan applications in physics, the materials sciences and for SEM generally.

Acknowledgements

The support of the Science and Engineering Research Council, technical assistance from Micro Consultants Ltd, and considerable help from Prof Sir Peter Hirsch FRS are gratefully acknowledged and Miss Diane Taylor is thanked for processing the manuscript.

References

1. E D Boyes et al 38th Ann.Proc.EMSA, (1980) 226.
2. E D Boyes, B J Muggridge and M J Goringe, J of Micros. 127 (1982) 321.
3. Micro Consultants Ltd, Kenley, Surrey.
4. E D Boyes Nature 304 (1983) 289.
5. G R Sawyer and T F Page J.of.Mat.Sci. 13 (1978) 885.

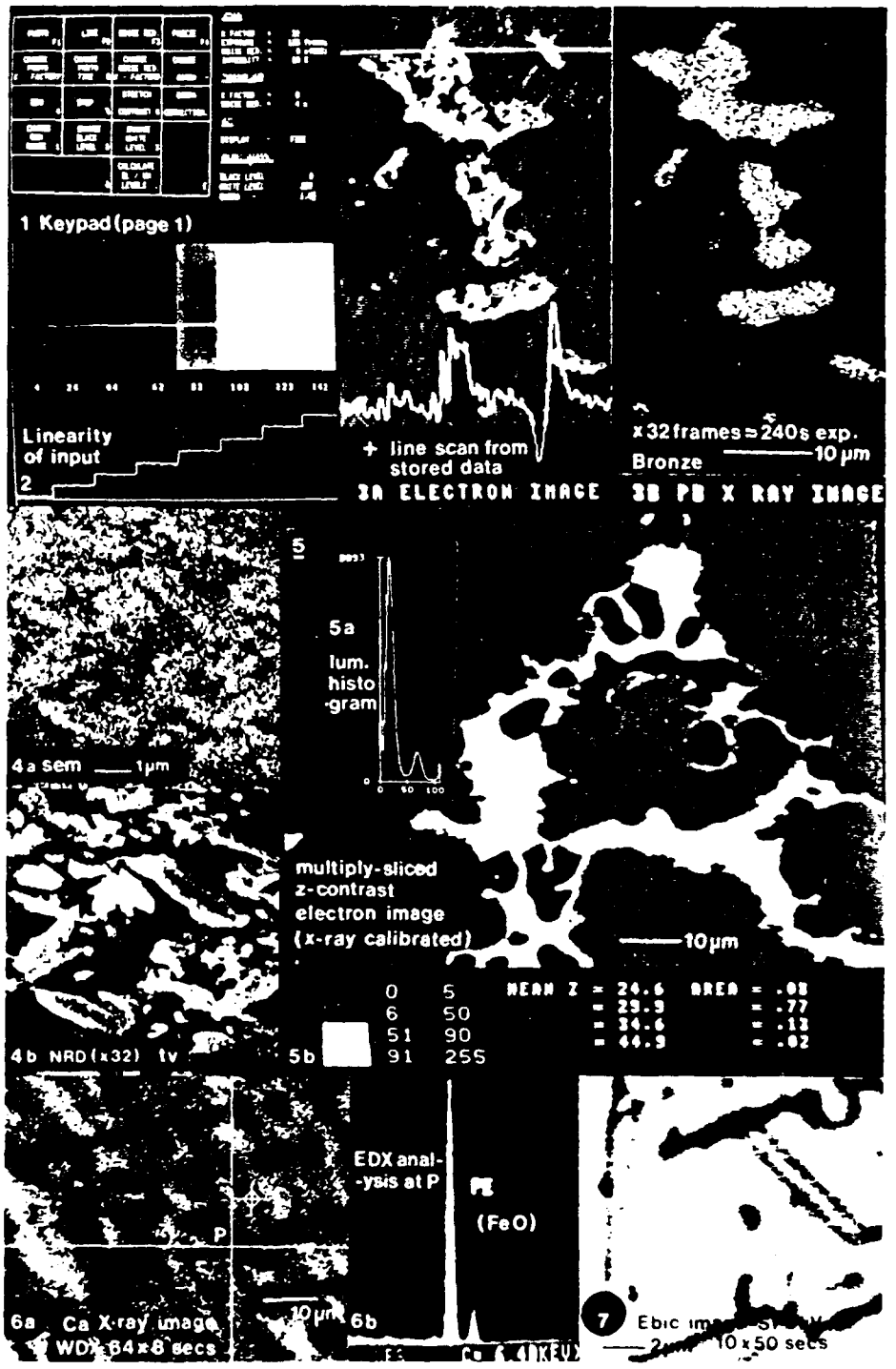
1 Keypad (page 1)
Linearity of input
2
+ line scan from stored data
3A ELECTRON IMAGE
x32 frames ≈ 240s exp.
Bronze
10 μm
3B PB X RAY IMAGE
4a sem
1μm
5
5a lum. histo -gram
multiply-sliced z-contrast electron image (x-ray calibrated)
10μm
0 5
6 50
51 90
91 255
5b
MEAN Z = 24.6 AREA = .08
= 28.9 = .77
= 34.6 = .13
= 44.9 = .02
4b NRD (x32) tv
EDX anal- -ysis at P
P
Fe
(FeO)
6a Ca X-ray image
WD: 84x8 secs
10μm
6b
7
Ebic im
10 x 50 secs

G. W. Bailey, Ed. *Proceedings of the 42nd Annual Meeting of the Electron Microscopy Society of America*

HIGH RESOLUTION AT LOW VOLTAGE : THE SEM PHILOSOPHER'S STONE?

E. D. Boyes

Department of Metallurgy & Science of Materials, University of Oxford, Parks Road, Oxford OX1 3PH, England

A new type of scanning electron microscope (SEM) has been designed to produce nanometre-level high resolution secondary electron images of the surfaces of uncoated non-conducting specimens such as structural ceramics, cement (Fig.1), supported catalyst particles (Fig.2), fine scale metallic features (Fig.3) including radiation damage, and eventually also biological material[1-2]. Clean low voltage systems also look promising for micro-analysis of surface layers e.g. Fig.4.

Very useful 5-20nm resolution images of surfaces are obtained[3-5] with a conventional electron microscope operated at 25-100kV (Figs.2,3) but at these high accelerating voltages the secondary electron yield of most materials is very low[6], typically < 0.1, and there are therefore severe surface charging problems with non-conducting regions of specimens, the images of which are consequently of poor quality. Conversely at very low voltages of 0.1-3kV secondary electron yields are high and generally close to unity minimising charging but the electron-optical performance of the conventional microscope is then limited to a resolution of 0.1 micrometres (100nm) or more. There may well be other operational limitations associated with the aperture dependent probe current, susceptibility to external AC magnetic fields, contamination of microscope and specimen etc[7].

In many practical applications the traditional solution to this dilemma is to use high voltages and coat the specimens with a conductive film of carbon or metal to control charging, but this reduces the potential for high resolution surface information and may complicate any subsequent microanalysis e.g. of battery aluminas or cement-based materials. They preclude looking at supported metal particle catalysts[8] (a major potential application) and must be avoided if semiconductor devices are to be operated diagnostically or after a quality control evaluation[9]. At the highest resolution coatings may introduce a characteristic surface texture of their own[10]. It is a bit like interpreting the image of a country-side scene after a snow storm: some features are enhanced or even revealed by shadowing/drifting, some are modified and others lost altogether. High voltage beam breakthrough or image blooming at the edge of features can lead to serious errors in assessment and metrology[11].

The LVSEM is designed to improve the low voltage imaging performance sufficiently to eliminate the need to coat samples and should make it possible to observe fine scale topogragphy directly, as well as utilising potential contrast effects[12] of secondary emission dependent on crystal structure orientation, surface chemistry and other work function variations[13]. Images obtained at low voltage are significantly more surface localised with reductions in the excitation volume (Fig.4) and in the effective spread of the beam interaction generally; largely eliminating the secondary background due to backscattered electrons[14] and restricting the beam breakthrough at surface steps or thin layers, enhancing contrast. As a consequence the image resolution of sharp features at low voltage should be very similar to the probe size, which is not always the case at higher voltages[1,5].

The secondary electron production efficiency is optimised at low voltages, improving the signal for a given probe current by an order of magnitude or more and largely compensating for the lower specific brightness (β.V) of

the gun under these conditions. Between the V_1/V_2 cross-over potentials the total electron yield is stabilised at unity by a small positive potential generated on the surface to maintain a local charge equilibrium. This negative feedback is related to the work function and at typically less than one volt is otherwise insignificant. The precise energies, including V_1/V_2, depend sensitively on the material and treatment of each specimen[5-11]. In this region contrast lies in variations in the purely secondary electron emission. The detector should therefore be designed to filter subsidiary backscattered electron (BSE) induced effects together with the BSE signal itself. Energy selected backscattered electrons have been used most effectively for high resolution imaging of surface topography[17] and defects[18].

The theoretical performance of an electron probe system with an optimised source can be described by an equation of the type:-

$$d = A\sqrt{\left(\frac{4i}{\beta V.\pi^2\alpha^2}\right) + \left(\tfrac{1}{4}C_s\alpha^3\right)^2 + \left(C_c\frac{\Delta V}{V}\alpha\right)^2 + \left(\frac{0.61\lambda}{\alpha}\right)^2} \qquad (1)$$

or

$$d = A\sqrt{(B + S^2 + C^2 + D^2)} \qquad (2)$$

where C_s and C_c are respectively the spherical and chromatic aberration coefficents, α is the probe semi-angle (Sr), β is the effective source brightness ($A/cm^2/Sr/volt$), V and ΔV are the accelerating voltage and energy spread of the beam and λ is the electron wavelength corresponding to V. Probe currents (i) of 1×10^{-11} A (10pA#1) and 1pA(#2) were used in the calculations. The smaller currents correspond to optimum recording conditions with good contrast specimens at high voltages. They may be more practical with the bigger signals available at low voltages and by using a digital imaging system. The 10-90% risetime at an edge can be better than the point resolution ($A = 1$) by a factor of ~ 3, depending on the current and its distribution. These values ($A = 0.3$) are also of interest as an accepted SEM resolution test. Each term has a dependence on both accelerating voltage (V) and aperture semi-angle (α), but in practice it is desirable to select V independently to optimise the interaction with the specimen and to maximise the current by choosing the largest aperture consistent with acceptable geometrical aberrations for a given magnification. At high voltages spherical aberration dominates but as the voltage is reduced the chromatic and brightness terms becoming increasingly important.

A re-examination of the electron-optical principles involved[8,19-21] has shown that with a minimum of component innovation it is possible to design a new type of LVSEM instrument which avoids most of the main problems by providing a projected low voltage (~ 1kV) resolution in the nanometre range and fully comparable to that achieved with conventional SEMs at high voltage.

The essential features of the new instrument are the combination of a high brightness and low energy spread field emission gun (FEG) operating at up to 30kV with a high quality lens and stage assembly in a very short (6cm), mechanically rigid and magnetically well screened column. Inadvertant coating of the specimens is controlled by providing a clean ion pumped vacuum system equipped with a cryobaffle and a prepumped airlock. The differentially pumped gun chamber is fully UHV (10^{-10} torr) and the whole system is bakeable. Operation of the field emitter at voltages down to 0.1kV whilst retaining the 1-5kV(+) extraction bias will be assisted by superimposing the magnetic field from a co-axial minilens focussing system. Scanning is phase synchronised.

At low voltages (V < 10kV) very high relative excitations of $NI/V_r \sim 30$ can

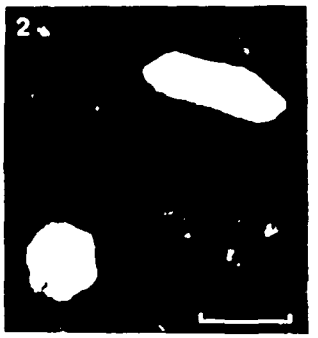

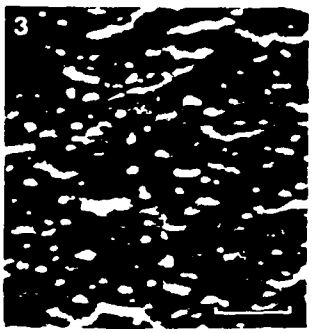

Fig.1. Defect in cement imaged uncoated without charging at 1kV. (Scale is 0.1mm)
Fig.2. Crystallographic surface platinum metal particles in supported Pt/Al_2O_3 catalyst (ref.8) TEM/SEM. (Scale is 0.1μm)
Fig.3. High resolution of low contrast < 20nm precipitates in Al-Si alloy, TEM/SEM at 100kV. (Scale is 0.2μm)

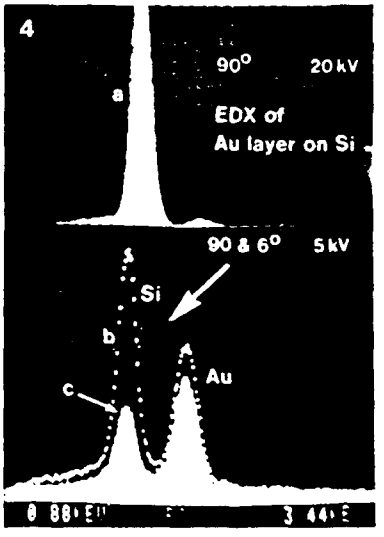

Fig.4. The effect of excitation volume as a function of kV; using X-rays (EDX) from a composite specimen with ~ 10nm Au layer on Si. (a) 20kV normal (90°) incidence - very small Au signal; (b) 5kV at 90° - substantial signal from Au surface film; (c) 5kV at glancing incidence of 6° (semi-RHEED conditions with penetration equivalent to 500V at 90°) - Au signal is dominant peak in spectrum: beam energy still sufficient to excite Au(M) and Si(K). The lack of Au/Si ratio sensitivity to tilt in the range 3-6° indicates mixed Si-Au surface with island formation or alloying between the elements.

easily be used at modest NI and power loadings with magnetic fields (~ 1T) well below saturation le els. Extremely low aberration coefficients (e.g. C_s = 0.27cm, C_c = 0.4mm) are possible in a conventional (non-superconducting) symmetrical condenser-objective probe lens operated in enhanced second-zone mode[22]. Secondary electron collection is highly efficient[23] with space for specimens up to a few millimetres in thickness and a size limited solely by the bore of the current airlock/stage system. The practically important aperture condition is also relaxed. The electron-optical aperture is still very small compared to the optical microscope, preserving a useful but not unlimited depth of field.

Fig.5.
SEM/LVSEM performance calculations (with A = 1)

S1: Regular SEM
C_s=75mm, C_c=20mm
β(W) = 2A/cm^2/Sr/V
ΔV=2.5eV, 1x10^{-11} A (10pA)

S2: as #1 (both tungsten thermionic gun)
1x10^{-12} A (1pA)

L1: LVSEM #1
C_s=0.99mm, C_c=0.94mm
β(FEG)=1000A/cm^2/Sr/V
ΔV=0.5eV, 1x10^{-11} A

L2: LVSEM #2,
C_s=0.27mm, C_c=0.4mm
β(FEG) = 1000A/cm^2/Sr/V
ΔV=0.2eV, 1x10^{-12}A

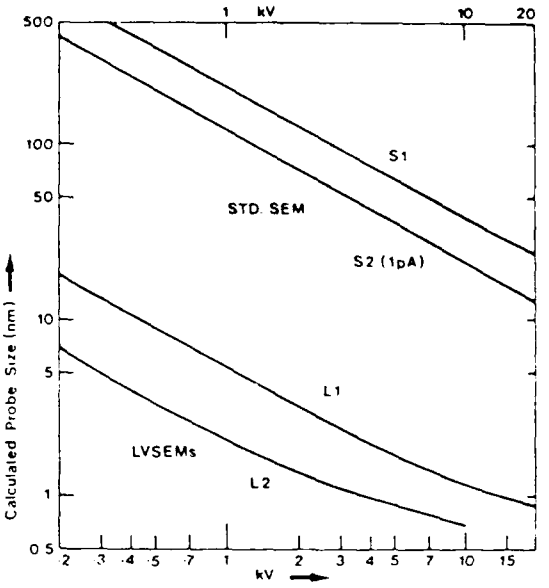

This work has been made possible by a grant (DAJA 37-82-C-0271)from the European Research Office of the US Army with additional support from the Science and Engineering Research Council (UK). Professor Sir Peter Hirsch FRS is thanked for many valuable discussions and for the provision of facilities; Stephen Thoms for assistance with lens calculations and Diane Taylor for processing the manuscript.

1. E.D. Boyes, Inst.Phys.Conf.Ser. 61 (1982) 27.
2. J.B. Pawley and M.P. Winters, Proc. 41st Ann. EMSA (1983) 488.
3. R.F.W. Pease and W.C. Nixon, J.Sci.Instr. 42 (1965) 81.
4. A.N. Broers, J.Vac.Sci.Technol, 10 (1973) 979.
5. C.J. Catto and K.C.A. Smith, J.Microsc. 98 (1973) 417.
6. L. Reimer and C. Tollkamp, Scanning 3 (1980) 35.
7. A.P. Wilska, J. Microsc., 83 (1964) 207.
8. P.J.F. Harris and E.D. Boyes, Inst.Phys.Conf.Ser., 68 (1984) 275.
9. K. Ura, Hitachi Instrument News 5 (1980) 2.
10. B.J. Panessa-Warren and A.N. Broers, Ultramicrosc., 4 (1979) 317.
11. V. Coates, Proc. 40th Ann. EMSA (1982) 752.
12. G.R. Sawyer and T.F. Page, J.Mater.Sci., 13 (1978) 885.
13. M. Hanbrucken, M. Futamoto and J.A. Venables, IOP, 68 (1984) 135.
14. L.M. Welter and V.J. Coates, SEM/1974, 59.
15. P.H. Dawson, J.Appl.Phys., 37 (1966) 3644.
16. Y. Ishikawa et al, Surface Science, 124 (1983) 87.
17. O.C. Wells, A.N. Broers and C.G. Bremer, Appl.Phys.Lett., 23 (1974) 353.
18. P. Morin et al, Phil.Mag., A40 (1979) 511.
19. A.V. Crewe, Ultramicrosc., 1 (1976) 267.
20. J.E. Barth and J.B. LePoole, Ultramicrosc., 1 (1976) 387.
21. N. Tamura et al, Electron Microsc., 1 (1980) 520.
22. W. Kamminga, Optik, 45 (1976) 39.
23. H. Koike, K. Ueno and M. Suzuki, Proc. 29th Ann. EMSA (1971) 28.

Cathodoluminescence of catalyst crystallites

E. D. Boyes*, P. L. Gai* & C. Warwick†

* Department of Metallurgy and Science of Materials, University of Oxford, Parks Road, Oxford OX1 3PH, UK
† RSRE, St Andrews Road, Malvern, Worcs WR14 3PS, UK

Heterogeneous catalysis has played a major role in the development of the chemical industry[1]. Metal oxide catalysts, for example, are used in selective oxidation and ammoxidation of hydrocarbons to produce key industrial chemicals. The activity and selectivity of such catalysts are greatly influenced by their microstructural and electronic structure changes under operating conditions. Here we report the first investigation of the electronic properties of small selected areas of catalyst particles, each only a few micrometers in extent, using a scanning electron microscope technique originally developed for characterizing semiconductor materials. The wavelength of the light emitted by selective electron probe stimulation (cathodoluminescence) can be directly related to the local bandgap energy of the material and the intensity of the signal to the point defect level. Some interpretation is required, but there are minimal specimen preparation requirements and the process is essentially non-destructive so that development sequences can be followed. In favourable cases the important aggregations of point defects can be mapped with respect to other microstructural features. An electronic contribution to promoter mechanisms is suggested.

Certain extended defects, for example, crystallographic shear (CS) defects introduced into some oxide catalysts to accommodate the non-stoichiometry (a result of the loss of lattice oxygen for catalysis) are thought to be relevant for oxygen exchange and catalytic activity in selective oxidation reactions[2]. However, operation without such defects has been established for commercially important Te and Bi molybdate systems under operating conditions using a combination of *in situ* (dynamic) electron microscopy (EM), high resolution EM and analytical EM (AEM)[3,4]. Direct studies coupled with parallel chemical experiments on some model catalyst systems, for example MoO_3 and V_2O_5, have also indicated that the CS defects in these play only a limited role in the reactions[5], suggesting that they are a consequence or an accommodation of the changes produced by the catalytic activity (for example, an accommodation of supersaturation of vacancies), rather than the origin of reactivity.

From the studies on model as well as commercial catalyst systems it is clear therefore that in addition to microstructural changes, point defect density and electronic structure can both have a significant influence on the chemical properties and hence on the effectiveness of the material as a catalyst. Scanning electron microscopy (SEM) and probe techniques commonly applied to semiconductor materials[6,7] have been used to examine this and to supplement information from *in situ* EM, ultra-high resolution structure imaging, conventional AEM and electron probe chemical microanalysis (EPMA)[8]. The initial emphasis has been to use cathodoluminescence, which, unlike electron beam induced conductivity, is a non-contacting technique and does not have any special specimen requirements. It is limited to bandgaps in the optical range (1–5 eV), but this covers many of the materials of interest. Experiments are possible with very small, usually single crystal, particles only a few micrometres in size, and generally very similar to the catalyst samples used in practical applications. The large single crystals required by more conventional methods for determining electronic properties are not usually available for these complex powdered catalyst materials (and with large single crystals it is difficult to obtain the relevant products by reaction under realistic conditions). The data available in the literature[9] are consequently very incomplete, precluding comparison with theoretical calculations[10] and perhaps resulting in an over-emphasis on structural

Reprinted from Nature, Vol 313, No 6004, pp 666-668, 21 February 1985
Macmillan Journals Ltd, 1985

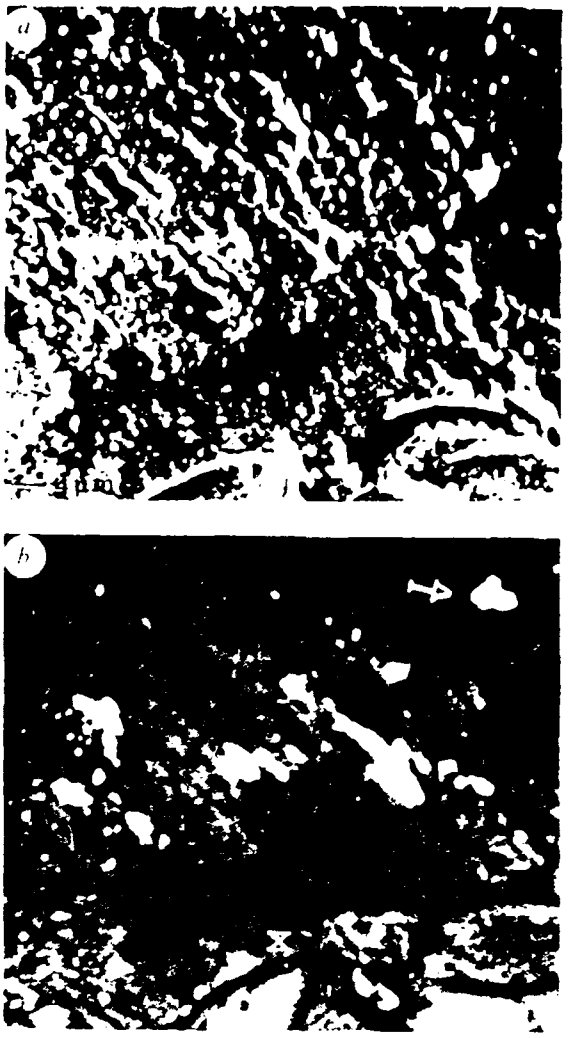

Fig. 1 Reduced TiO_2. *a*, SEM image; *b*, cathodoluminescence image. Liquid N_2 temperatures were used.

factors in evaluating catalytic compounds.

Experiments were carried out on materials of interest in catalysis, namely, rutile (TiO_2), mixed Sn/Sb oxides and Bi molybdate systems. The TiO_2 powder was crushed from a boule (National Lead Company, USA)[11]; the mixed Sn/Sb oxide catalyst powders were prepared by co-precipitation using appropriate amounts of $SnCl_4$ and Sb/aqueous ammoniacal solution; Bi molybdate powders were prepared by co-precipitating aqueous Bi nitrate and ammonium para-molybdate solutions[3]. The catalyst particles were several micrometres in extent in each case and were dispersed on the usual carbon support films for microscopy. Reduction experiments were performed on the catalysts (using (111) rutile and Sn/Sb oxide crystallites and (001) Bi molybdate), *in situ*, in a high voltage EM (an AEI-EM7 HVEM) fitted with a gas reaction cell[4], in a controlled H_2 environment and at operating temperatures, with and without the electron beam, to obtain the reaction sequences. Parallel experiments were also performed outside the HVEM in a gas reaction chamber connected to a mass spectrometer and a gas chromatograph, to confirm the direct studies. Cathodoluminescence experiments were carried out on both fresh and reacted specimens using a Cambridge Stereoscan SEM fitted with a cathodoluminescence detector and operating at 30 keV. A combination of an elliptical mirror and light guide was used to collect the cathodoluminescence with reasonable efficiency. It could be connected either directly to a suitable photomultiplier for the total signal or through an optical spectrometer, which

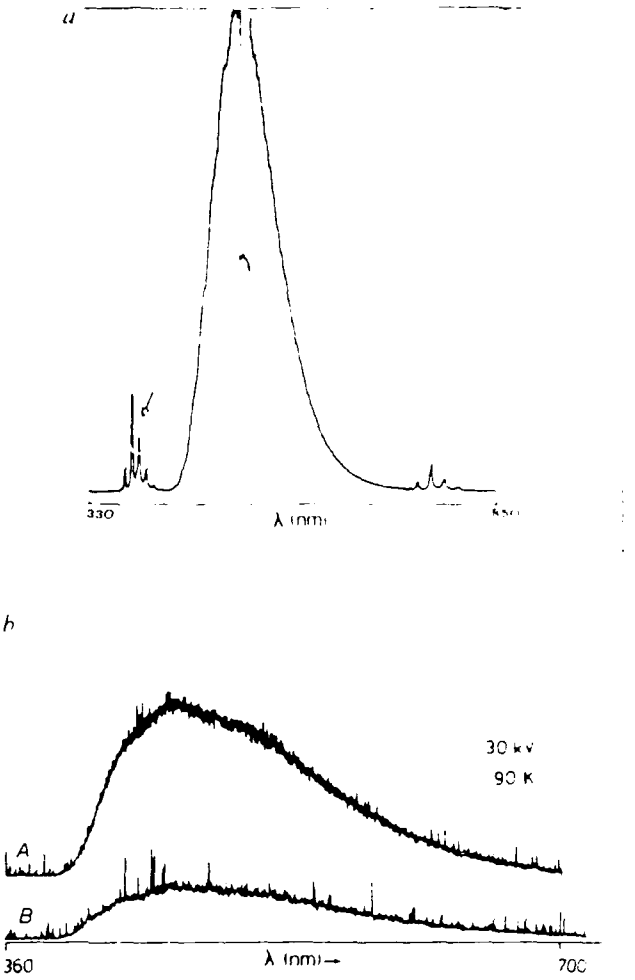

Fig. 2 *a*, Cathodoluminescence spectrum of pure ZnO, showing the potential of the technique. The bandgap is 3 eV (arrowed) but donor levels (of 0.3 eV) below the conduction band create additional charge carriers. *b*, Spectra from two regions of reduced TiO_2, each 10 μm^2. *A* is from a bright region (as arrowed in Fig. 1) and *B* is from a background region. The difference is mainly owing to point defects. The peak occurs at 465 nm (2.67 eV).

was scanned to produce the analytical spectra[1-3].

In general, the prepared materials produced relatively uniform images in both SEM (secondary electron image and back-scattered electrons and cathodoluminescence), which were interpreted as coming from smooth and homogeneous surfaces. After reaction, considerable surface roughness was often imaged in the SEM as shown in Fig. 1*a* for rutile reduced at 850 °C; notable and unexpected cathodoluminescence contrast effects were obtained (Fig. 1*b*), which cannot be readily explained by the observed structural defects or surface topography, that is, they are not well correlated with the SEM images from the same areas. Figure 1*b* illustrates sharply defined patches of bright contrast and also the darker inverse (with respect to the background level).

The energy of the cathodoluminescence signal is a function of the bandgap for the appropriate transition between electron energy states in the material. Using this technique, it has been possible to confirm already known bandgaps[4], for example, ~3 eV for ZnO (Fig. 2*a*) and 3.2-3.5 eV for TiO_2 used as a support for catalysts, and to establish completely unknown electron energy levels from the emission colour and spectra of small reacted crystallites of TiO_2, even from the selected ~10-μm^2 regions shown in Fig. 2*b*. Cathodoluminescence experiments have also been useful in the interpretation of catalytic

Fig. 3 SEM image of Sn/Sb oxide catalyst reduced in H_2, indicating surface segregation of species

behaviour of complex mixed Sn/Sb oxide (with 0.7 atom % Sb) catalysts.

In situ H_2-reduction experiments carried out on the catalyst system in the HVEM show no extended CS defects at operating temperatures. The SEM images of the reacted specimen shown in Fig. 3 indicate considerable complexity, with in this case evidence for segregation of species on the surface. The cathodoluminescence spectra of the reacted and unreacted specimens reveal marked differences as shown in Fig. 4*A* and *B* respectively, with band gaps of 2.6 eV and 1.9 eV, suggesting variations in composition. The EPMA quantitative analysis shows depletion of Sb in the bulk (0.2 atom % Sb in the bulk) and, therefore, possible surface segregation of Sb. This work has also produced the first estimates of bandgap energy of ~2 eV for Bi_2MoO_6 (γ-bismuth molybdate), which is the commercially important catalyst in the selective oxidation/ammoxidation of propylene to acrolein/acrylonitrile used for resins and fibres[3]. This energy (2 eV) is conveniently in the visible region of the spectrum.

The energy and intensity of the cathodoluminescence signal is influenced by structural features that modify electronic properties including the generation of defects and new phases under operating conditions. The allowed electron energy levels can be expected to be changed by the presence of the defects. If discrete levels, perhaps associated with structural changes, are involved, a different and diagnostic wavelength of radiation may be produced. Point defects can introduce a continuous range of degenerate levels leading to broadening of the emission

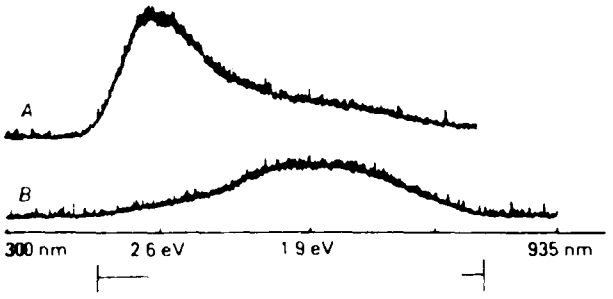

Fig. 4 Cathodoluminescence spectra of *A*, the reacted Sn/Sb oxide catalyst and *B*, the unreacted catalyst, showing a peak shift indicative of chemical or structural change.

peaks (for example, Fig. 2*b*) and to a progressive and non-radiative quenching of the diffusing carrier species before a radiative recombination process can occur. Alternatively, point defects may act as carrier traps, enhancing the probability of radiative recombination in a way similar to activators in phosphors and dopants in light emitting diodes. This might also be one role of the promoters present in many commerical catalysts and could help to explain the mechanism by which they are effective.

The image contrast obtained with cathodoluminescence can thus be used to examine the distribution of moderate to low levels of point defects in the matrix, and in the presence of more extended defects, which are believed to play a major role in both binding of reaction species and in diffusion through the bulk between the reaction sites. To minimize the introduction of additional point defects, cathodoluminescence microscopy was always performed before other examinations at higher voltages. More efficient cathodoluminescence detection should reduce the beam current requirements and the risk of any artefact effects being induced under vacuum in the SEM. All the cathodoluminescence results have been obtained with normal incidence at 30 keV. Lower voltages and operation with glancing incidence in a manner analogous to reflection high-energy electron diffraction (RHEED) should permit more surface localized analysis, although there will also be enhanced recombination at the surface, which will reduce intensities.

The results should assist in the explanation and prediction of the catalytic properties of some complex and not well understood but commerically important materials.

We thank the SERC for support.

Received 8 May; accepted 19 December 1984

1 Hucknall, D. J. in *Selective Oxidation of Hydrocarbons* (Academic, New York, 1974)
2 Stone, F. S. *J. Solid State Chem.* **12**, 271–283 (1975)
3 Gai, P. L., Boyes, E. D. & Bart, J. C. J. *Phil. Mag.* **A45**, 531–547 (1982)
4 Gai, P. L. *J. Solid State Chem.* **49**, 25–42 (1983)
5 Gai, P. L. *Phil. Mag.* **A43**, 841–857 (1981)
6 Holt, D. B. *Inst. Phys. (Lond.) Conf. Ser.* **60**, 165–178 (1981)
7 Booker, G. R. *Inst. Phys. (Lond.) Conf. Ser.* **60**, 203–214 (1981)
8 Boyes, E. D. & Gai, P. L. *Proceedings of AEM workshop, Microbeam Analytical Society Vail* (ed. Geiss, R.) 71–75 (San Francisco Press, San Francisco, 1981)
9 Rao, C. N. R. & Subbarao, G. V. *Phys. Stat. Sol.* **A1**, 597–614 (1970)
10 Blanchin, M., Bursill, L. A., Hutchison, J. & Gai, P. L. *J. Physique* **42**, 95–110 (1981)
11 Mackrodt, W. C. in *Computer Simulation in the Physics and Chemistry of Solids*, 71–82 (Daresbury Laboratory, 1980)
12 Warwick, C. A. & Booker, G. R. *Inst. Phys. Conf. Ser.* **67**, 321–326 (1983)

Inst. Phys. Conf. Ser. No 78: Chapter 7
Paper presented at EMAG '85, Newcastle upon Tyne, 2-5 September 1985

Sub-micron backscattered electron microanalysis in the SEM

E D Boyes, M D Hill, M J Goringe and C J Salter,
Department of Metallurgy and Science of Materials, University of Oxford, Parks Road, Oxford OX1 3PH.

The use of bulk specimens has many practical advantages. They should be more representative of the material; simpler to prepare and with fewer artefacts. Features which are more widely spaced or with a lower frequency of occurrence than can be readily handled in a typical transmission electron microscope (TEM) specimen with an open area which may be no more than a few micrometers in diameter, can be analysed quite simply with the wide field of view available in the scanning electron microscope (SEM). The specimens should be more robust and therefore suitable for ongoing experiments such as heating or the attachment of the connections needed to operate devices. However a major disadvantage of electron opaque specimens is the relatively poor micron sized spatial resolution and hence reduced sensitivity of chemical analysis by X-ray spectrometry; particularly when compared with the sub-nanometer, and in the most favourable cases sub-monolayer, capability demonstrated with EDX analysis of thin foils in the FEG STEM. In extreme cases, of relatively high energies and light matrices, the resolution may be many micrometers. Diffraction contrast analysis of defects is also less well developed. On the other hand, when fully quantitative corrections are applied to the data the chemical microanalysis of bulk specimen is inherently more accurate ; due principly to the better defined physics.

It is well established that :-

(a) there is a strong energy dependence to the range of electron beam interaction with a bulk specimen and a lower voltage means less spreading,

(b) for any given element there is a minimum energy below which the excitation of characteristic x-rays is inefficient,

(c) the range and hence the degree of lateral spreading is much reduced for those electrons which are backscattered with sufficient energy to be re-emitted through the entrance surface,

(d) the yield of backscattered electrons (BSE) from a polished sample at normal incidence is a monotonic function of atomic number, and simple rules of mixture govern the yield from alloys and materials of different density, including where there is porosity,

(e) the absolute yield of backscattered electrons is high - up to 0.5 - but the corresponding figures for x-rays are very much lower.

It is possible to construct highly efficient detectors for backscattered electrons, based on either a scintillator/photomultiplier or solid state diodes; with a very wide angle of acceptance of up to at least 1.7Sr, compared to 0.1Sr for a good EDX x-ray detector and much less for WDX. The efficiency of the method means that low beam currents of <0.5nA can be used for BSE analysis; minimising the probe size contribution to the overall resolution, and restricting the effects on beam sensitive specimens. Continuous digital analysis of the experimental data is used to control acquisition interactively (Fig.4) and to enhance the results, without corrupting the basic data which is securely stored digitally.

To highlight small differences, BSE microanalysis images are generally presented most usefully as false colour coded maps. Fig.2(c) is a monochrome reproduction of a high resolution BSE image, subjected to non-linear enhancement in which adjacent grey levels are assigned different colours. Under computer control it is possible to have multiple regions of interest. The data in the Fig.3 histogram were subsequently processed in this way. To do this effectively it is necessary to have extremely even illumination of the specimen and a high degree of uniformity in signal collection.

A number of minor perturbations in the Z dependence of the BSE signal have been reported, but within the restricted range of carefully prepared samples so far studied, reliable relative compositions have been consistently obtained : the data in Figs.1(d) & 2(a) are examples. Of course only in a binary material is the result unique, since in more complex compositions it is in principle possible to have more than one way of combining the constituents to attain any given mean Z, which forms the basis of this method of analysis. In practice there may be other beneficial constraints to the possible combinations, or as in Fig.2(b&c) one of the elements is constant.

The technique has the potential for accurately analysing and efficiently mapping the distribution of the major elements associated with future sub-micron microelectronic devices. Being proportional to the mean atomic number, it is insensitive to the minor elements. However it is particularly effective for materials, such as oxides, which contain the lighter elements; although for a given energy the spatial resolution is then more limited.

A DEC LSI-11/23 minicomputer has been used but the most useful functions of digital line traces and spot measurements of intensity, together with the necessary calibration and video expansion routines, could have been run almost as well on a low cost micro system. Chemically accurate images require a framestore with digitisation and storage to better than 8-bit precision. A high precision 12-bit ADC has been connected through the computer bus, bypassing the framestore's integral digitiser, and operating much more slowly. The earlier system required the analogue video signal to be controllably amplified in gain and offset to fit the restricted useful range of the 256 level 8-bit standard input digitiser. In practice this presented few problems with modern electronics, and the limiting stability is that of the SEM beam. This was addressed by using internal standards, as close to the target material as possible; and in all respects similar to the procedure used in EPMA, including EDX spot calibration for mean Z.

Some problems were experienced with attaining the necessary quality of surface finish to obtain a purely compositional BSE signal. The annular detector geometry does not entirely suppress the modification of the yield as a function of angle of incidence, although it copes well with any associated changes in angle of emission, which are successfully integrated out. We have used a JEOL 35X, which has been fitted with an original design of scintillator backscattered electron detector (to be published; M D Hill, Inst of Phys Conf Ser 76, 1985).

A lateral spatial resolution of 0.1μm and a chemical accuracy of 1% have been demonstrated for the analysis of mercury in CdHgTe using the calibrated and digitally processed integral backscattered electron signal from a regular SEM fitted with an efficient annular detector system. At Z = 60 the discrimination is better than 0.25AMU.

Fig.1 Alternate layers of GaAs, each 1.2μm wide, and 5.[illegible]m GaAlAs with different proportions of Ga/Al in multilayer cross-section specimen. The compositional BSE image has better resolution, despite the higher kV, and signal to noise ratio (S/N), than the X-ray map.

(a) Quantitative EPMA x-ray data

Ga	.09	.19	.30	.39	.50
Al	.44	.33	.21	.12	-
As	.47	.48	.49	.49	.50

(b) Al(Kα) X-ray map (4kV, 300secs).

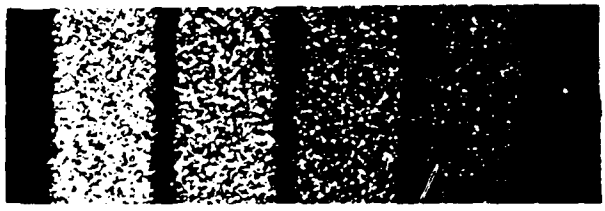

(c) Backscattered electron (BSE) image (15kV, 50s, compositional).

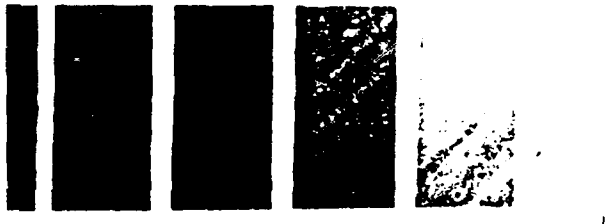

(d) Atomic number (mean Z, from (a) dependence of the electron backscattering

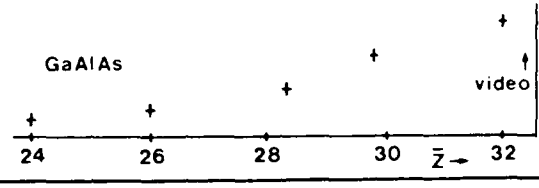

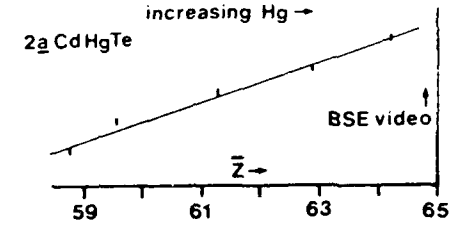

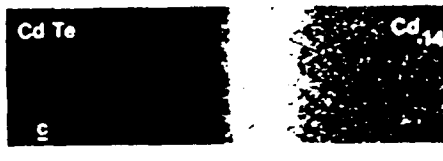

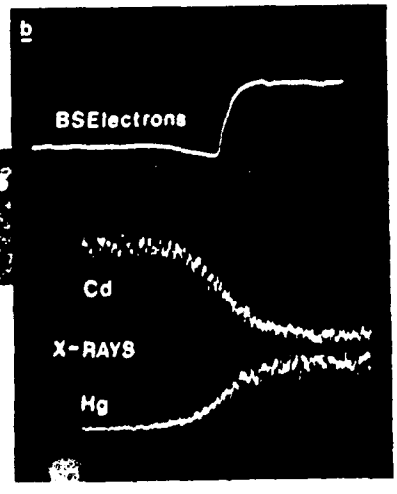

Fig.2 (a) Z-contrast from Cadmium Mercury Telluride compositions plotted against mean Z from EPMA X-ray data, with <0.25AMU discrimination at Z=60.
(b) Interface in CdTe/CdHgTe (line=5μm).
(c) BSE digital image of b (0.15μm bar) non-linear enhanced for colour.

Fig.3 Digital backscattered electron image of artificial sandstone with superimposed luminance histogram as basis for x,y,Z and area fraction image analysis.

INTERACTIVE DIGITAL IMAGING

Fig.4

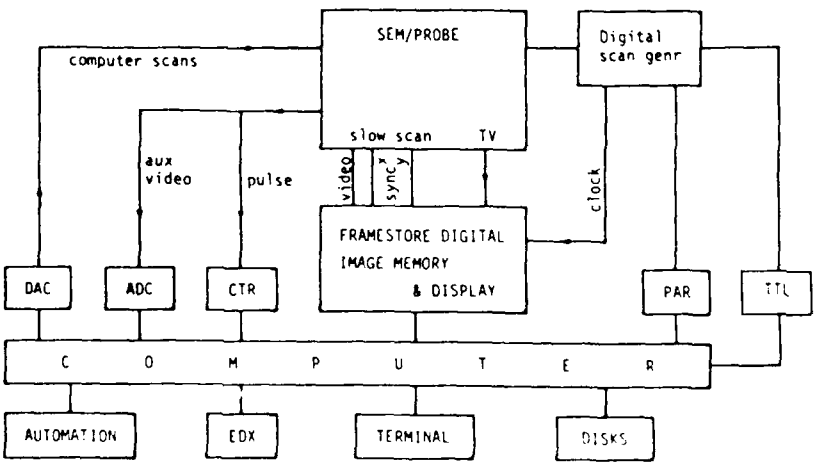

We thank the SERC and AERE Harwell for support. The semi-conductor specimens were provided by Dr G R Booker, M Lyster and Dr Astles (RSRE) and the sandstone by Dr S Graham of Shell Oil, to all of whom the authors are most grateful.

Abstract of invited keynote presentation at MICRO-86, organised by the Royal Microscopical Society, 1986, and published in the Society's Proceedings, July 1986.

THE POTENTIAL OF LOW VOLTAGE SCANNING ELECTRON MICROSCOPY (LVSEM)

E D Boyes

Department of Metallurgy and Science of Materials, University of Oxford, Parks Road, Oxford OX1 3PH.

There are major advantages in operating a scanning electron microscope at low voltages of 1kV or less. In general the total yield of secondary electrons is high and charging of unccated nonconducting specimens is therefore minimised. In addition the signal is more surface sensitive, with edges better delineated. There may also be less radiation damage. However under these conditions the resolution of the conventional SEM is quite limited, with a probe size of 0.1um or more, and for many applications it is necessary to use higher voltages and conductive coatings.

The SEM electron optics can be improved considerably, at the expense of some flexibility of operation, by using a second zone condenser objective lens with inherently low aberrations. At low voltages it is possible to use very high relative excitations (>200) without running into engineering problems, since the absolute values of current, cooling and saturation remain low (B<1T). This geometry is also advantageous for thicker specimens, and the low energy secondary electrons are collected efficiently, and selectively, as they spiral up through the lens. The dominant terms in the performance calculations are the chromatic aberrations of the lens (evaluated by the established Munro programs; in this case without saturation) and the (low) energy spread and high brightness of an LaB6 or field emission electron gun. The deleterious effects of AC fields can be minimised by a very short electron path length of <70mm, comprehensive double walled screening and the use of scanning systems phase locked to the local mains frequency.

The potential performance of the specialised LVSEM has been calculated. A lens with Cs <0.15mm and Cc <0.4mm is feasible in low voltage applications. It should be possible to achieve high performance in the instrument, with an edge resolution at <1kV of <<10nm, and perhaps eventually approaching 1nm and challenging the TEM in some applications; whilst using only existing technology.

Proc. XIth Int. Cong. on Electron Microscopy, Kyoto, 1986

THE POTENTIAL OF LOW VOLTAGE SCANNING ELECTRON MICROSCOPY (LVSEM)

E D BOYES

Department of Metallurgy and Science of Materials,
University of Oxford, Parks Road, Oxford OX1 3PH, England.

There are major advantages in operating a scanning electron microscope at low voltages of around 1kV. In general the total yield of secondary electrons is high and charging of uncoated nonconducting specimens is therefore minimised. In addition the signal is more surface sensitive, with edges better delineated. However under these conditions the resolution of the conventional SEM is quite limited, with a probe size of 0.1um or more, and for many applications it is necessary to use higher voltages and conductive coatings.

The SEM electron optics can be improved considerably, at the expense of some flexibility of operation, by using a second zone condenser objective lens with inherently low aberrations. At low voltages it is possible to use very high relative excitations without running into engineering problems, since the absolute values of current, cooling and saturation remain low (B<1T). This geometry is also advantageous for thicker specimens, and the low energy secondary electrons are collected efficiently, and selectively, as they spiral up through the lens. The dominant terms in the performance calculations are the chromatic aberrations of the lens (evaluated by the established Munro programs; in this case without saturation) and the low energy spread and high brightness of the essential field emission electron gun. The effects of AC fields can be minimised by a very short electron path length of 70mm, comprehensive double walled screening, selection of a suitable site for the instrument and scanning systems phase locked to the local mains frequency. Both TV rate scanning and digital slow scan are framestore processed, principaly to improve statistics. There are clean vacuum systems and a prepumped airlock.

The potential performance of the specialised LVSEM has been calculated (Fig.2) on the basis of using for both the lens and gun technology which is already established in other applications, but has not previously been used for an SEM. It has been shown (Fig.1) that a lens with Cs <0.15mm and Cc <0.4mm is feasible in this low voltage application. For practical reasons a better overall performance may be obtained with rather higher values. It is found that the practically important aperture condition is relaxed somewhat. However the depth of field is useful, but restricted, with an optimum aperture. It seems that it should be possible to realise a practical LVSEM specification with a performance approaching an edge resolution of 1nm at 1kV, using only existing technology. It would open up important new applications in ceramic science, catalysis, radiation damage, surface studies and potentially also in the biological sciences.

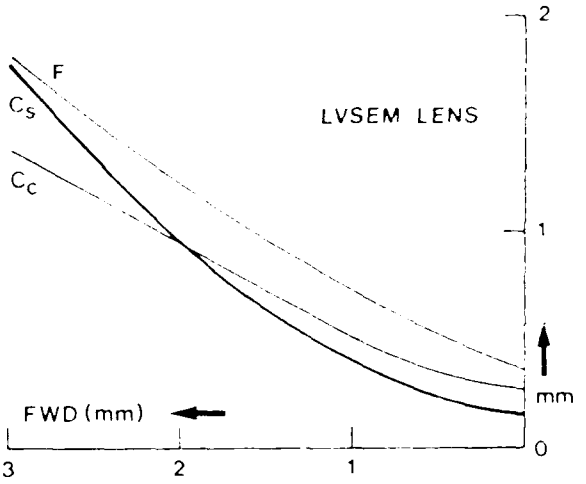

Fig.1 LVSEM lens properties calculated as a function of the free working distance (FWD) between the specimen and the upper polepiece (immersion lens). F=focal length, Cs=spherical, and Cc= chromatic aberration coefficients (mm). Munro program.

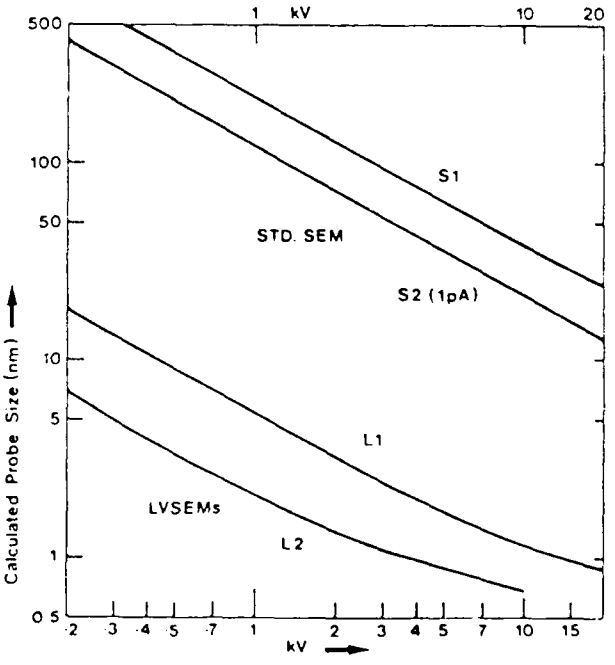

Fig.2 Performance estimates for various SEM/LVSEM specifications.

S1: Regular SEM
C_S=75mm, C_C=20mm
β(W) = 2A/cm^2/Sr/V
ΔV=2.5eV, 1x10^{-11} A (10pA)

S2: as #1 (both tungsten thermionic gun)
1x10^{-12} A (1pA)

L1: LVSEM #1
C_S=0.99mm, C_C=0.94mm
β(FEG)=1000A/cm^2/Sr/V
ΔV=0.5eV, 1x10^{-11} A

L2: LVSEM #2,
C_S=0.27mm, C_C=0.4mm
β(FEG) = 1000A/cm^2/Sr/V
ΔV=0.2eV, 1x10^{-12}A

Inst. Phys. Conf. Ser. No. 90: Chapter 9 307
Paper presented at EMAG 87, Manchester, 8-9 September 1987

Microstructures of high T_c Y-Ba Cu-O superconductors

P L Gai, S E Male (*), C J Salter, N J Long and F D Boyes

Department of Metallurgy and Science of Materials, University of Oxford, and (*) Central Electricity Research Laboratories (CEGB), Leatherhead.

The discovery of superconductivity at elevated critical temperatures (Tc), above that of liquid nitrogen, in the complex Y-Ba-Cu oxides based on the oxygen deficient 1-2-3 phase YBa2Cu3O7-x (fig.1, JEOL 4000EX) has great importance. The classical metallic alloy superconductors have Tc values below 24K, necessitating the use of expensive liquid helium or hydrogen cryogen systems. In retrospect it can be seen that the earlier results from some oxides of lead were also anomalous, but the importance of this was not fully appreciated at the time. The breakthrough came much more recently (Bednorz and Muller, 1986) with the discovery of superconductivity at around 40K in the LaBaCu oxides. The properties of the Y compounds (Wu et al, 1987) are even better, with Tc typically >90K, and they have therefore superceded the earlier materials. A wide range of other complex oxides have now been examined and it may be possible to achieve even higher Tc values.

There has been a parallel effort to characterise the microstructures (eg Male et al, 1987) of the materials since they are also important in practical applications. Whilst the critical temperature (Tc) is determined principally by the crystal chemistry, including oxygen deficiency, and crystal structure; the current carrying capacity (Jc) depends critically on the microstructure and grain boundary character, in terms of appropriate flux pinning centres, porosity and general interconnectivity of the material. The overall microstructure has been refined, with a corresponding reduction in the level of defects, including the high density of microtwins in the initial 1-2-3 crystals, and an improvement in the geometric interconnectivity whilst retaining the desirable crystal chemistry and hence Tc properties of the oxide (Tc = 91.5+/-1K). It is clearly necessary to understand and creatively control critical aspects of the microstructural development of these materials.

They were prepared by mixing appropriate amounts of Y2O3, BaCO3 and CuO powders, which were pressed at 2 GPa and solid state reacted by heating in air at 950C for 12 hours. Most of the samples were then quenched, reground etc and annealed in flowing oxygen for various times (0 to 80 hours) at 900C. This procedure inevitably results in considerable porosity (27%), which reduces the cross-sectional area of the grain to grain contacts and limits the potential Jc. Although the microstructures can be extensively modified by appropriate processing, eg figs.2 & 3, the density remains at 73%. The preliminary data from the ragged structure of the lightly annealed material (fig.2) has a measured Jc of >100A/cm2 at 77K under zero field conditions, whilst the modified material oxygen

annealed for 30 hours (fig.3), which has a much lower room temperature resistivity, also has a rather lower measured Jc (fig.5). However the Tc transition is sharpened by longer heat treatments in air or by extended oxygen annealing, which is consistent with the production of a cleaner material. It should be noted that substantial corrections may have to be applied to Jc data, but not necessarily to Tc, measured from a porous compacted specimen; and there may be additional problems with the gold evaporated/silver dag four point probe contacts used for the Jc measurements, indicative of the enabling technologies which will be necessary for exploitation. The high resolution SEM of this 30-hour annealed sample (fig.4) also illustrates aspects of the growth of a generally cleaner microstructure with pseudo-sintering bridges between adjacent grains and the extensive area of compact grain boundary contact. The nature of the porosity, but not the overall amount (27%), of porosity was markedly changed, with voids typically smaller and more uniform in size, and more rounded in shape. Some facetting and as yet unidentified 10nm-scale features on the surface of the 1-2-3 grains appear to be oriented with respect to the underlying crystal structure. It seems that at this stage of development the nature of the grain boundaries, in terms of crystallography and structure, and the incidence of other defects, may be more important than the simple geometric interconnectivity. We plan to develop schemes of controlled precipitation to provide independent flux-pinning centres. The aim is to produce a homogeneous structure with clean grain boundaries without amorphous layers, which would be expected to destroy the superconductivity. Sections microtomed or crushed, but not ion-thinned, generally have high angle grain boundaries with direct crystal-to-crystal contact and no evidence for any amorphous intermediate layers, even on the atomic scale at a triple point (fig.6), or by microanalysis.

Parallel electron diffraction and EDX microanalysis (fig.7) of crushed samples in the Cu-free environment of the Philips CM12 AEM with Be grids in a Be holder, and EPMA (Cameca) of polished bulk specimens; confirmed that oxygen annealing the almost 100% $YBa_2Cu_3O_{7-x}$ starting material for 30 hours produced 3% of the morphologically distinctive semiconducting 2-1-1 oxide Y_2BaCuO_5 as separate rounded grains rather than as intergrowths. The EPMA analysis gave 6.85+/-0.10 for the oxygen content, in line with other techniques. EELS (fig.8) using the VG STEM with a 1nm/1nA probe showed the expected Ba(M) edge typical of Ba2+ but a delayed and rounded Cu(L) edge not expected from any identifiable oxidised Cu state, but resembling a 'metallic' bandstructure. The edge shapes did not change as a function of orientation or electron irradiation dose; the diffraction pattern was maintained and the very large O(K) peak in the spectrum (fig.9) from the Link high sensitivity (0.18Sr) windowless EDX detector was not significantly reduced during EELS data acquisition from the approximately 30nm thick crystal (and two surface zones), suggesting that the data can be attributed to the native crystal and not to any obvious artefacts. The materials and properties were stable and reproducible.

Bednorz J G and Muller K A, Z Phys B64, 189 (1986).
Wu M K et al, Phys Rev Lett 58, 908 (1987).
Male S E, Gai P L and Boyes E D, European Conference on High Tc Superconductors, Genoa, July 1987.

We thank the SERC for supporting PLG, NJL and some of the EM facilities.

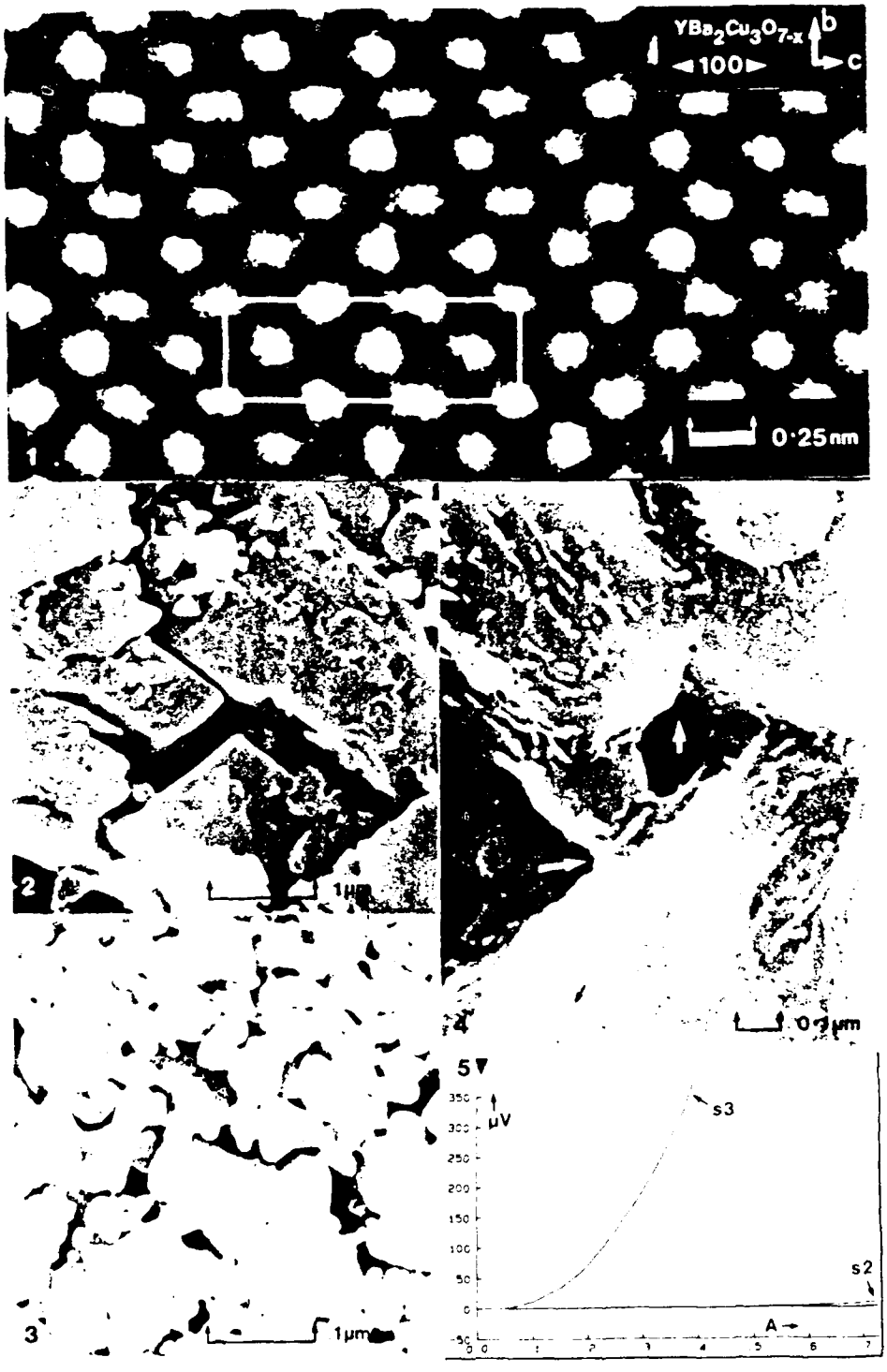
$YBa_2Cu_3O_{7-x}$
b
c
100
0·25nm
1
2
1μm
3
1μm
4
0·1μm
5
μV
s3
s2
A
350
300
250
200
150
100
50
0
-50
0
1
2
3
4
5
6
7


2·5nm

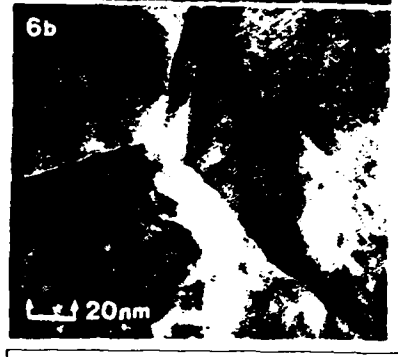
6b
20nm

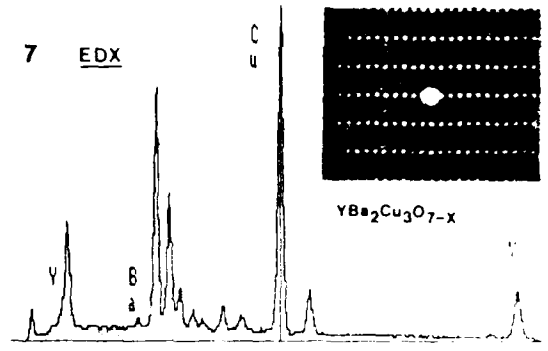
7
EDX
Cu
Ba
Y
$YBa_2Cu_3O_{7-X}$

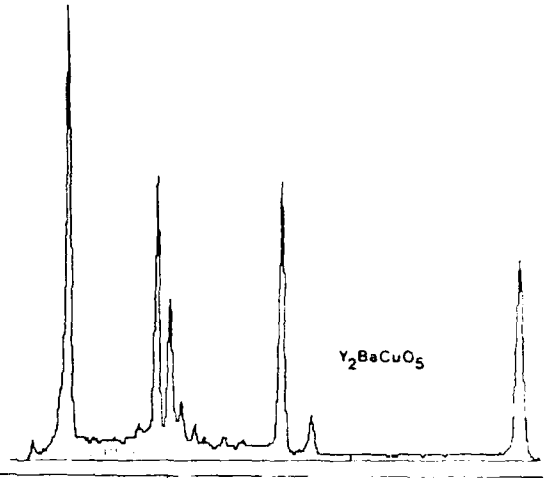
Y_2BaCuO_5

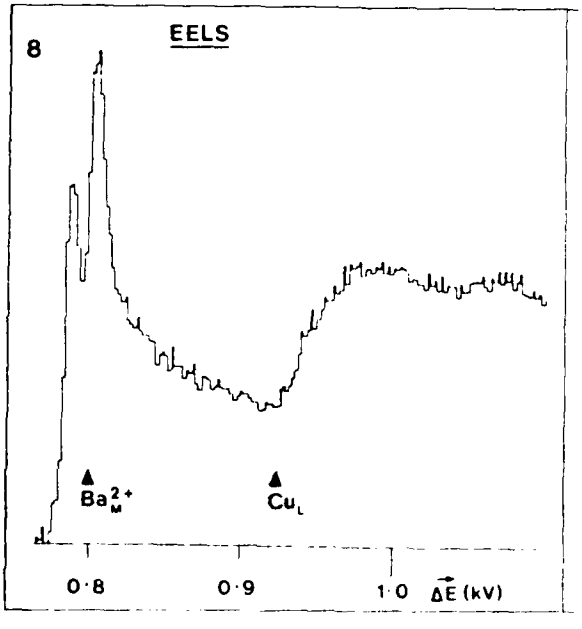
8
EELS
Ba^{2+}_M
Cu_L
0·8
0·9
1·0
ΔE (kV)

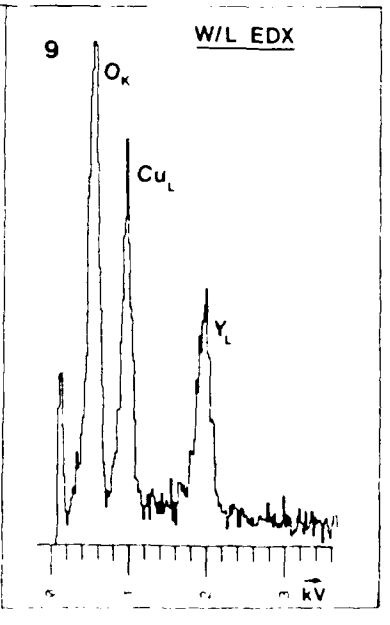
9
W/L EDX
O_K
Cu_L
Y_L
kV